1 **A Review of Fluid Inclusion Constraints on Mineralization in the Irish Orefield**

2 **and Implications for the Genesis of Sediment-Hosted Zn-Pb deposits**

3

4 J.J. Wilkinson

5

6 CODES, University of Tasmania, Private Bag 126, Hobart, Tasmania 7001, Australia

7

8 and

9

10 Department of Earth Science and Engineering, Imperial College London, South Kensington Campus,

11 Exhibition Road, London SW7 2AZ, UK

12

13

14 **Abstract**

15

16 Many fluid inclusion studies have been carried out in the Irish Midlands Basin orefield (Lower

17 Carboniferous) since the earliest work by Ed Roedder in the late 1960s. Results show that, in the ore

18 deposits, the total range in fluid salinity is 4-28 wt% NaCl equivalent but with the majority falling in

19 the moderate salinity range between 8-19 wt%. This variability is interpreted in terms of mixing

20 between moderate salinity ore fluids and low temperature brines during ore formation. The most

21 northerly ore deposits of Navan and Abbeytown are distinct in containing fluids of both lower and

22 higher salinity than is typical of the Waulsortian-hosted deposits further south (Tynagh, Silvermines,

23 Lisheen and Galmoy). Subeconomic prospects tend to display a narrower range in salinity, mostly at

24 the lower end of the range observed in the ore deposits. In some prospects, and on the margins of

25 some ore deposits, evidence for dilution is observed, interpreted to reflect mixing between

26 hydrothermal fluids and unmodified seawater. This process is inferred to be unfavorable for

27 mineralization.

28   Homogenization temperatures, a reasonable proxy for true trapping temperatures in the orefield,

29 range from 70-280 °C but with the majority falling between 130-240 °C. There is no evidence for

30 systematic stretching or leakage of inclusions related to the post-entrapment heating implied by

31 elevated thermal maturity indicators. The highest temperatures are observed in the Waulsortian-

32 hosted systems, with peak temperatures of ~280 °C supported by local, high grade Cu and Ni

33 mineralization. In the Navan and Abbeytown deposits, lower temperature fluids appear to have been

34 more prevalent. The subeconomic prospects formed over essentially the same temperature range as

35 the ore deposits (90-270 °C), with the exception of the morphologically and texturally distinct MVT

36 systems in the region (e.g., Kinnitty, Harberton Bridge) that formed at lower temperatures (50-100

37 °C).

38   Similar hydrothermal fluids to those recorded in both deposits and prospects are widely observed

39 in dolomite (and sometimes calcite) cements within Courceyan-Arundian age rocks indicating

40 hydrothermal fluid activity occurred over an extremely large area (>30,000 km^2) and probably over

41 an extended time period. There is a broad regional division in fluid properties suggesting that the

42 northwestern and southeastern provinces, separated by the trace of the Iapetus suture zone, may

43 represent partly decoupled, large-scale flow regimes. Up to three, low temperature brine types are

44 also recorded by cements in the host rock sequence, indicating a complex range of evaporation and

45 fluid-rock interaction processes were ongoing in the shallow basin succession during the period of

46 hydrothermal activity.

47   Halogen data show that fluids involved in mineralization were originally seawater-derived brines,

48 produced by evaporation to varying degrees. Relatively high temperature, basement-interacted

49 hydrothermal fluids were derived from partially evaporated seawater (molar Cl/Br = 559-825). Their

50 compositions can be explained by dolomitization in the Carboniferous succession prior to circulation

51 to depth; alkali exchange, reduction and metal-leaching from the Lower Paleozoic basement; and

52 mixing with low temperature brines that locally penetrated the upper parts of the basement rock

53 package. Fertile ore fluids appear to be characterized by higher δ^{18}O (+7 to +9 ‰), lower δD (-25 to -

54 45 ‰) and much higher metal contents than otherwise similar fluids sampled in basement-hosted

55 feeder veins distal to deposits. This may reflect highly efficient metal scavenging in deeper/higher

56 temperature reaction zones that underlie the principal deposits. In the ore deposits, these fluids

57 mixed with Br-enriched bittern brines (Cl/Br ~290) produced by evaporation of Carboniferous

58 seawater past halite saturation. It is inferred that bittern brine generation occurred in the shallow

59 marine shelf regions in the footwalls to the synsedimentary fault systems that controlled the

60 localization of mineralization. These brines then migrated into hangingwall depressions where they

61 ponded within permeable sediments and became enriched in H_2S via bacteriogenic sulfate reduction.

62 The coincidence of structurally-controlled, high temperature reaction zones, brine-producing

63 footwalls, and hangingwall traps, with bacterial blooms above upwelling plumes of hydrothermal

64 fluids, can be interpreted as a self-organizing system that locally converged on ore-forming

65 conditions. Understanding the first-order structural control of the ore systems will therefore be

66 critical for predicting new deposits.

67   The Irish orefield presents arguably the best database available on the thermal and chemical

68 characteristics of hydrothermal fluids involved in sediment-hosted ore genesis. The system shares

69 much of the variety and complexity observed in other intracratonic basin-hosted Zn-Pb(-Ba) ore

70   districts. This includes the coexistence of contrasting styles of mineralization that are typically

71   observed in the more distal and platform-marginal parts of the basinal environment. The thermal

72   and chemical fluid heterogeneity observed is typical of modern intracratonic basin systems and

73   should be expected in large paleohydrothermal systems where recharge of surface-derived fluids is

74   involved.

75

76   **Introduction**

77

78   The Carboniferous Irish Midlands Basin hosts a remarkable concentration of base metals (~17 MT

79   known) in a prospective area of approximately 200x150 km. In addition to the known prospects,

80   operating mines at Navan, Lisheen and Galmoy, and the historical mines at Tynagh, Silvermines and

81   Abbeytown, anomalous concentrations of Zn and Pb are common in the lower part of the

82   Waulsortian Limestone Formation and pervasive in the Navan Group – the primary host rock

83   sequences (Blakeman, pers. comm.). Such extensive mineralization implies the operation of a giant

84   hydrothermal system of significant academic as well as economic interest. Indeed, the orefield has

85   been important in a number of debates on the classification of sediment-hosted deposits and the

86   nature of the hydrothermal systems that form them (Russell, 1978; Russell et al., 1981; Hitzman and

87   Large, 1986; Lydon, 1986; Hitzman and Beaty, 1996; Everett et al., 2003; Wilkinson, 2003; Leach et

88   al., 2005; Wilkinson et al., 2005a).

89   The purpose of this paper is to provide a historical review of fluid inclusion studies carried out in

90   the Irish orefield, including investigations of individual mineralized systems (deposits and prospects)

91   as well as regional studies in the host rock stratigraphy and underlying basement. The contribution of

92   these data to the development of genetic models for mineralization is highlighted. Previously

93   unpublished data are also presented that, in combination with the published results, provide an

94   extensive dataset that constrains the nature of the fluid regimes operating in the region prior to,

95   during, and subsequent to the main stages of ore formation. How these data impact on our

96   understanding of the Irish paleohydrothermal system and the wider implications for models of

97   sediment-hosted ore formation are considered.

98

99   **Geological Setting and Mineralization**

100

101   A thorough description of the geology and mineralization in Ireland is beyond the scope of this

102   contribution and only a brief summary is presented here. For more detail and thorough reviews the

103   reader is referred to Andrew et al. (1986), Hitzman and Large (1986), Phillips and Sevastopulo (1986),

104   Bowden et al. (1992), Andrew (1993), Anderson et al. (1995), Hitzman (1995), Hitzman and Beaty

105   (1996), and Kelly et al. (2003).

106   Zinc-lead mineralization in the Irish Midlands is hosted by Lower Carboniferous (Dinantian)

107   carbonate rocks (Fig. 1), within both the Waulsortian Limestone Formation and the Navan Group –

108   the first major non-argillaceous carbonate units in a transgressive marine sequence. Beneath these

109   rocks lie red, terrestrial mudstones, sandstones and conglomerates (Old Red Sandstone, ORS) that in

110   turn unconformably overlie an eroded Lower Paleozoic volcanosedimentary succession that was

111   deformed and underwent low grade metamorphism in the Caledonian Orogeny. A crystalline

112   basement is inferred at depth in the Midlands area (Strogen, 1974; Kennan et al., 1979) and likely

113   comprises Grenvillian gneiss and schist to the northwest and late Precambrian, probably Avalonian,

114   gneissic rocks to the southeast (Watson, 1978; Phillips and Sevastopulo, 1986).

115   The Waulsortian Limestone Formation developed in a ramp environment in the Courceyan as

116   biomicrite mounds surrounded by argillaceous bioclastic limestones (ABL) at moderate water depths

117   of up to several hundred meters. Waulsortian banks dominate in the south and west Midlands,

118   where they coalesced to form thicknesses in excess of 750 m (Andrew, 1993) in the Shannon Trough

119   (Fig. 1). The Navan Group, of similar age, comprises near-shore, shallow marine, largely high-energy

120   deposits, including oolitic and bioclastic grainstones, birdseye micrites and minor sandstones

121   (Philcox, 1984). These were deposited in the northern Midlands on the southern margin of the

122   Laurasian landmass, now marked by the Longford Down inlier (Fig. 1).

123   The host rocks underwent early diagenesis that included extensive calcite cementation and

124   dolomitization (Lees and Miller, 1995; Rizzi and Braithwaite, 1997; Gregg et al., 2001; Lee and

125   Wilkinson, 2002; Wilkinson, 2003; Nagy et al., 2004). It is widely considered that these processes

126   were initated upon deposition of the carbonate sediments, with significant cementation occurring

127   within a few tens of meters of the seafloor (cf. Dix and Edwards, 1996). Early dolomitization is

128   pervasive in the southeastern Midlands, fringing the Leinster Massif (Phillips and Sevastopulo, 1986;

129   Hitzman and Beaty, 1996; Gregg et al., 2001; Nagy et al., 2004), but is also widely developed

130   elsewhere (Gregg et al., 2001). Sulfides appear to generally postdate early dolomite cements and are

131   themselves accompanied by a variety of replacive, breccia-cementing and vein- and vug-filling calcite

132   and dolomite, plus variable barite and minor quartz (Fig. 2).

133   Mineralization in the ore deposits principally occurs as massive sulfide displaying a complex range

134   of textures (Boast et al., 1981; Taylor, 1984; Ashton et al., 1986; Anderson et al., 1998; Hitzman et al.,

135   2002; Fusciardi et al., 2003; Lowther et al., 2003; Wilkinson et al., 2005b). In sub-economic

136   mineralization, a variety of massive, disseminated, breccia- and vein-filling styles occur (e.g.

137   Holdstock, 1982; Emo, 1986; Grennan, 1986; Trude and Wilkinson, 2001). Abundant ore minerals are

138   sphalerite, galena and pyrite, with lesser but variable marcasite and minor chalcopyrite, tennantite

139   and other sulfosalts. Orebodies are broadly stratiform but in most cases have been shown to be

140   strictly stratabound and occur as single or multiple lenses hosted by favorable horizons within the

141   hostrock packages. For the deposits of Lisheen and Galmoy, this is a breccia unit of variable

142   thickness, located close to the base of the Waulsortian Limestone.

143

The Reliability of Fluid Inclusion Data

145

146   A fundamental assumption in fluid inclusion studies is that inclusions have maintained their integrity

147   since their time of formation (Roedder, 1984). In the Irish Midlands, the validity of fluid inclusion

148   data has been questioned by some authors (Hitzman, 1995; Hitzman and Beaty, 1996; Peace, 1999;

149   Reed and Wallace, 2001) because vitrinite reflectance and conodont color analyses suggest that the

150   Carboniferous rocks have been subject to late Carboniferous heating (Clayton et al., 1989). The

151   highest maturation values are observed in the Munster Basin in southern Ireland where Variscan

152   deformation and metamorphism have occurred. However, high values extend into the southeast and

153   west Midlands where, taken at face value, vitrinite reflectance values (R_m >4%) imply peak

154   temperatures in excess of 300 °C and conodont alteration indices (CAI) of 5-7 imply temperatures of

155   300 to >550 °C. Any re-equilibration toward lower density (greater inclusion volume) by plastic

156   stretching, or partial leakage of inclusions, as a result of overheating would result in anomalously

157   high homogenization temperature (T_h) values and an overestimate of ore fluid temperatures. Thus,

158   although no textural evidence for inclusion re-equilibration (e.g. Bodnar, 2003a) has been described

159   from the Irish Midlands, it is nonetheless important to consider this issue before discussing the data

160   in detail.

161   Laboratory studies have shown that the potential for inclusion re-equilibration during overheating

162   is largely a function of inclusion size and host mineral strength (e.g. Bodnar and Bethke, 1984;

163   Burruss, 1987; Bodnar et al., 1989). Consequently, a plot of inclusion size against T_h should show a

164   positive correlation if partial re-equilibration has occurred and this effect would be more pronounced

165   for softer minerals in which inclusions can deform under lower internal overpressures (e.g. calcite,

166   barite). In addition, modification is more likely to affect some inclusions in a given inclusion

167   assemblage than others due to variations in size, shape, or proximity to defects. This would result in

168   variable T_h data within individual inclusion populations and the elimination of systematic differences

169   between different growth stages of a single mineral grain, or between different paragenetic stages.

170   The first application of a size/T_h test for different host minerals was presented by Everett et al.

171   (1999a) for data from Lower Paleozoic-hosted veins. These data are supplemented here and

172   compared with results from regional carbonates and deposits (Fig. 3A). For all datasets (with the

173   possible exception of deposit barite), no positive correlation is apparent for any mineral host.

174   Sphalerite and quartz are the strongest host minerals and therefore might be expected to preserve a

175   putative lower temperature population, especially in smaller inclusions. In fact, the opposite is

176   observed, with these minerals generally hosting higher T_h inclusions. The broad T_h differences

177   between the minerals (quartz>calcite>dolomite>pink dolomite) and the notable bimodality in

178   sphalerite values cannot be easily explained by re-equilibration and are likely to reflect features of

179   genetic significance, principally differences in precipitation temperature.

180   A similar plot for regional Lower Carboniferous carbonates (Fig. 3B) again shows no size-T_h

181   correlation, appears to show a bimodality in dolomite data, and illustrates low T_h values in the

182   weakest mineral, calcite.

183   For the deposit data, sphalerite T_h values are the highest, followed by dolomite and then calcite –

184   the opposite of what might be expected for stretching populations. At some of the prospects (e.g.

185   Harberton Bridge; Trude and Wilkinson, 2001) calcite hosts monophase inclusions that could not

186   have been preserved if post-entrapment temperatures had exceeded 300 °C. Barite also contains

187   monophase inclusions at some localities (e.g. Silvermines; Samson and Russell, 1987) that would be

188   impossible to preserve during such overheating. However, variable degrees of filling are commonly

189   observed in barite and a weak positive correlation between size and T_h is observed in the deposit

190   data (Fig. 3C) suggesting leakage (during post-entrapment burial or laboratory analysis) is a problem

191   for this mineral. Consequently, T_h data (but not necessarily compositional information) from barite

192   are treated as generally unreliable (cf. Bodnar and Bethke, 1984; Ulrich and Bodnar, 1988).

193   The last, and perhaps most convincing, evidence for preservation of inclusion integrity is the

194   petrography which demonstrates that individual inclusion populations (such as within a single

195   dolomite growth zone) typically display a relatively narrow range of T_h values that is much less than

196   within a sample as a whole, or between samples. Furthermore, systematic variations in

197   microthermometric data can be observed that relate to changes in fluid properties during crystal

198   growth (Fig. 4). These features would not be preserved if post-entrapment re-equilibration was

199   widespread.

200   The contradiction between Devonian and Carboniferous maturation data and Lower

201   Carboniferous fluid inclusion data is problematic. Although higher temperatures are plausible in the

202   Munster Basin to the south, where the rocks have been subjected to Variscan thrusting and have

203   developed a cleavage, it is difficult to credit rock temperatures of up to 550 °C in the Midlands Basin,

204   (except immediately adjacent to minor intrusions) given the lack of evidence for recrystallization at

205   such high temperatures, lack of mineralogical indicators, and perfect preservation of delicate fossils

206   and low-temperature diagenetic fabrics. Consequently, it has been suggested that CAI and R_m values

207   recorded in the Midlands do not reflect true maximum temperatures (Everett, 1999; Wilkinson et al.,

208   2003). The reason for this is uncertain, although it is most likely due to hydrothermal overprinting

209   (e.g. Rejebian et al. 1987) by the unusually extensive flow that has affected much of the stratigraphy

210   in the Midlands area, and which may have been active over a long period of time (e.g. Hitzman, 1995;

211   Wright et al. 2000; Gregg et al. 2001; Wilkinson, 2003).

212   The modification of CAI values by fluids is suggested by a number of features of the dataset

213   presented by Clayton et al. (1989). In particular, reddened limestones, commonly inferred to be

214   related to hydrothermal activity (Hitzman et al., 1995), display elevated CAI values of 6-7 compared

215   with values of 5-5.5 in normal limestones from the same drillhole or nearby (e.g. Meelin No.1

216   borehole, Co. Cork; Rocky Island, Co. Cork; Fig. 1). Also, dolomitized intervals can display higher CAI

217   than undolomitized intervals in the same drillhole (e.g. Ballyragget No. 1 borehole, Co. Kilkenny) and

218   there is often a variation of up to 1 CAI in single samples. Local vertical reversals in thermal gradients

219   down boreholes also suggest a complex thermal regime probably involving advective heating

220   (Goodhue and Clayton, 1999). This conclusion is supported by Jones (1992) who noted that CAI

221   values in Ireland are influenced by proximity to major mineral deposits and follow Caledonoid trends,

222   these structures also being implicated as the major infrabasinal flow conduits. Numerical modeling

223   has shown that anomalous organic maturity can be accounted for by free thermal convection in the

224   continental crust beneath intracratonic basins (Nunn, 1994). Consequently, the weight of evidence

225   supports widespread preservation of fluid inclusion integrity in the Midlands area and therefore in

226   the discussion below T_h values are considered reliable except where standard petrographic evidence

227   indicates otherwise.

228

229

230   **Historical Review of Fluid Inclusion Studies**

231

232   Fluid inclusion studies in the Irish orefield have played an important part in the development of

233   genetic models and the debate surrounding the timing and depth of mineralization. Opposing views

234   can be distilled down to purely epigenetic models invoking largely lateral fluid flow and replacement/

235   cavity-filling mineralization at depth, during burial, from fluids close to thermal equilibrium with their

236   host rocks (Hitzman and Beaty, 1996; Reed and Wallace, 2001; Peace et al., 2003); and SEDEX

237   models, in which near-seafloor and underlying epigenetic mineralization occurred during diagenesis

238   of the host rocks from elevated temperature fluids in the updrafts of a convective flow system

239   (Boyce et al., 1983; Russell, 1978, 1986). The more recent evidence that much mineralization

240   probably formed by host rock replacement in the shallow sub-seafloor environment (Anderson et al.,

241   1998; Blakeman et al., 2002; Lee and Wilkinson, 2002; Wilkinson et al., 2003, 2005a, 2005b) and a

242   relaxed definition of the term "SEDEX" (Leach et al., 2005) means that the deposits can be classified

243   as carbonate-replacement SEDEX type.

244   In the following review, only fluid inclusions interpreted to be of primary (or pseudosecondary)

245   origin and constrained paragenetically to be associated with the principal mineralizing stages are

246   considered, except where otherwise stated. In the summary of fluid properties (Table 1), the modes

247   and ranges given are considered to be the best reliable estimates based on published information;

248   these may omit outlying data which are noted and, in some cases, have necessitated a degree of

249   interpretation of results that may be equivocal. Most of the results discussed are salinity data

250   inferred from final ice melting (as the last solid phase), or in some cases hydrate melting

251   temperatures ($T_m$hyd), together with T_h values which, in the Irish system, can be considered to be a

252   reasonable proxy for trapping temperatures (e.g. Wilkinson and Earls, 2000). Additional chemical or

253   isotopic data acquired from fluid inclusion analyses are also discussed.

254

255   *Ore Deposits*

256   It is appropriate for this volume that the history of fluid inclusion research in Ireland was started

257   by Ed Roedder himself in the late 1960s. The earliest data reported, obtained on sphalerite from the

258   Keel deposit (Fig. 1), are attributed variously in the literature but were in fact acquired by Ed Roedder

259   (unpublished USGS memorandum to T.B. Nolan, 1968), listed in Roedder (1976), on samples

260   collected by Nolan on a visit to the deposit. Patterson (1970) cites these data and quotes from

261   Roedder's report:

262

263   *"The samples had clear euhedral, yellow to brown, unzoned sphalerite crystals up to 8 mm as a crust*

264   *on [Lower Paleozoic] quartzite. These sphalerite crystals contained reasonably good primary and*

265   *pseudo secondary fluid inclusions yielding the following data: (no distinction in the measurements*

266   *could be made between the two types of inclusions):*

267

268   *Freezing temperatures:*   *10 inclusions all between -7.35 ± 0.5 and -8.0 ± 0.2 °C*

269   *1 inclusion -6.0 ± 0.1 °C*

270   *Filling [homogenization] temperature:* *3 inclusions 176 ± 5 °C*

271   *5 inclusions 185 ± 3 °C*

272

273   *Thus* <u>*this sample*</u> *(if not the whole deposit), formed from rather hot brines, with a salinity in the range*

274   *of 11-12 per cent salts in solution."*

275

276   These were the first data to shed light on the nature of the fluids responsible for formation of the

277   Irish deposits and suggested that they formed at higher temperatures and from lower salinity fluids

278   than those typical of carbonate-hosted deposits of Mississippi Valley-type (MVT).

279   Early results were also reported by Greig et al. (1971) from Silvermines. Only three datapoints

280   (possibly averages of individual samples) were presented on a plot of T_h vs. distance from the

281   Silvermines fault zone; these indicated T_h values of 190-280 °C for inclusions hosted by quartz,

282   sphalerite and barite. Further reconnaissance results were presented by Probert (1983; cited in

283   Andrew, 1993) from locations in the northern Midlands including the Navan deposit and the Keel,

284   Moyvoughly and Tatestown prospects (Fig. 1). The absence of paragenetic or spatial control makes

285   interpretation of these results risky, but some comparisons with subsequent studies can be made

286   (Table 1). More recent and carefully-constrained results from Navan (this study) do not replicate

287   these early measurements although it should be noted that the high grade core of the deposit was

288   mined out in the 1980s-1990s.

289   *Silvermines:* The first detailed fluid inclusion study was carried out principally on the lower

290   (epigenetic) orebodies and Old Red Sandstone-hosted footwall veins from the Silvermines deposit

291   (Samson, 1983; Samson and Russell, 1983). Homogenization temperature and salinity data (modelled

292   in the NaCl-H_2O system) were reported from inferred primary and pseudosecondary liquid-vapor

293   fluid inclusions in quartz, sphalerite, calcite and dolomite, and salinity data from the predominantly

294   monophase liquid inclusions in barite. Extended results, including the addition of the first bulk

295   analytical (crush-leach) chemical and isotopic (decrepitation, crushing) data and the observation and

296   identification of trapped phases (calcite) in some inclusions were presented in a comprehensive,

297   benchmark study by Samson and Russell (1987).

298   Wide ranges in microthermometric properties were observed (Table 1) and the occurrence of

299   some vapor-rich inclusions in quartz was taken as evidence for episodic boiling; similar inclusions in

300   carbonate and barite were discounted. Since then, vapor-rich inclusions have not been reported

301   from the orefield (apart from in one Lower Paleozoic basement-hosted vein sample; Everett et al.,

302   1999a) so it is likely that boiling was not a common process in the district (Wilkinson et al., 2003). A

303   broad negative correlation between T_h and salinity was interpreted as the first direct evidence for

304   fluid mixing in the Irish deposits, previously suggested based on sulfur isotope data and the chemical

305   conditions of sulfide deposition (Boast et al., 1981). An important detail within this correlation is that

306   samples from different geographic locations and paleodepths within the system tend to fall in

307   different parts of the array, consistent with a relatively stable mixing zone between higher

308   temperature, less saline fluids at depth (and possibly also on the fringes of the system) and more

309   saline, cooler fluids higher up and in the center, proximal to the main ore zones.

310   *Tynagh:* Tynagh, the first Zn-Pb deposit to be discovered in the Lower Carboniferous of the

311   Midlands Basin, was the subject of a fluid inclusion study by Banks and Russell (1992). Primary and

312   secondary inclusion data were reported from limestone-hosted vein sphalerite from epigenetic

313   mineralization in Zones 2 and 3, the principal ore zones in the deposit (Boast et al., 1981), together

314   with results from barite (monophase liquid inclusions predominant) and quartz (Table 1). Quartz-

315   hosted inclusions were measured both from rare, euhedral quartz replacing carbonates in the ore

316   zones and in quartz overgrowths in the ORS within 1 m of the Tynagh Fault in the deposit footwall.

317   Although there is some ambiguity in the timing of these overgrowths, the inclusions were interpreted

318   as relating to the main stages of ore formation.

319   As with Silvermines, a negative correlation was observed between T_h and salinity in the inferred

320   ore-stage fluids, interpreted in terms of fluid mixing. The principal spread in salinities occurs in the

321   footwall quartz overgrowths and in barite implying that these either formed during mixing, and/or

322   were overprinted by fluids undergoing mixing. By contrast, and similar to Silvermines, the sphalerite

323   data show little spread in salinity suggesting precipitation under somewhat different conditions. Data

324   from quartz within the ores were not fully reported.

325   Banks and Russell (1992) also presented data from "post-ore" calcites that hosted four inclusion

326   types. Because the paragenesis of the samples and the petrography of the inclusions within them are

327   not described it is difficult to interpret these results. However, their Group 1 fluid inclusions (T_h 109-

328   196 °C; salinity 5.1-10.2 wt% NaCl equivalent; $T_m$hyd -24.9 to -22.4 °C) coincide with the data

329   reported by Probert (1983), as well as ore-stage fluids elsewhere (Table 1), and are therefore

330   considered likely to be related to mineralization, although this was discounted by the authors. Some

331   of the calcite samples were associated with a dolomite-chalcopyrite assemblage typical of the post-

332   ore pink dolomite and later calcite widely developed in the Midlands Basin (the D_5 and C_6 of

333   Wilkinson et al., 2005b; Fig. 2). This "copper dolomite" event is interpreted to represent a basin-wide

334   brine migration, probably related to the onset, or relaxation, of Variscan compression (Andrew,

335   1993; Wilkinson, 2003; Wilkinson et al., 2005b). The Group 3 inclusions of Banks and Russell (1992)

336   are potentially associated with this stage based on similarities with microthermometric data from

337   pink dolomite elsewhere (e.g. Eyre, 1998; Wilkinson, 2003). The Group 4 inclusions contained low

338   salinity fluids and displayed anomalous hydrate melting behavior, with hydrate and ice coexisting

339   above -20.8 °C, interpreted in terms of sulfate or bicarbonate presence. These are comparable to the

340   dilute fluids typical of the C_6 cement stage (Fig. 2) that are strongly oxidizing and may therefore

341   reflect groundwaters enriched in sulfate, possibly locally as a result of sulfide oxidation.

342   *Abbeytown:* The historic small mine of Abbeytown in Co. Sligo, studied by Hitzman (1986), lies

343   well to the northwest of the main orefield (Fig. 1) and its genetic relationship to it remains enigmatic.

344   A small number of two-phase fluid inclusions were analysed by R.J. Bodnar (cited in Hitzman, 1986)

345   from the main mineralizing stage (sphalerite and calcite) and from late ore-stage calcite-pyrite

346   breccias. These predominantly showed moderate salinities of 10-13 wt% NaCl equivalent, salinities

347   that are typical of ore-related inclusions throughout the Midlands Basin. T_h values varied from 85-180

348   °C with the majority in calcite falling at the upper end of this range and those in sphalerite at the

349   lower end. A minor population of more saline inclusions was also observed in ore-stage calcite but

350   their timing was not discussed. No evidence for fluid mixing was observed and it was suggested that

351   mineralization probably formed from a single fluid, perhaps due to cooling and/or neutralization by

352   hostrock dissolution.

353   *Lisheen:* The discovery of Galmoy in 1986 (Doyle et al., 1992) focused exploration attention on the

354   Rathdowney Trend in the southeast Midlands (Fig. 1), and proved a significant factor in the

355   subsequent discovery of the Lisheen deposit (Hitzman et al., 1992). Initial fluid inclusion studies were

356   reported in conference abstracts (Thompson et al., 1992; Eyre et al., 1996), with the first detailed

357   results presented by Eyre (1998). In this study, fluid inclusion analyses from Galmoy, Lisheen and a

358   number of prospects in the Rathdowney Trend were constrained with respect to the mineral

359   paragenesis observed in the samples (see Wilkinson et al., 2005b for details), synthesized in Figure 2.

360   All analyzed fluid inclusions from Lisheen were of liquid-vapor type and showed simple low

361   temperature phase behavior with first melting temperatures in the range -54 to -39 °C, best

362   interpreted in terms of the NaCl-CaCl$_2$-H$_2$O system. Fluid inclusions in sphalerite showing permissive

363   evidence for a primary origin displayed T$_m$hyd of -22.6 ± 0.3 °C indicating the dominance of NaCl (e.g.,

364   see Bodnar, 2003b). These yielded salinities mostly in the range 10.2-18.0 wt% NaCl equivalent. A

365   marked polymodal distribution of salinities was observed (Table 1), including an unusually low

366   salinity grouping from the outlying North Zone (Wilkinson et al., 2005b). Liquid-vapor

367   homogenization temperatures (to the liquid) were mainly in the range 140-210 °C (up to 241 °C) with

368   the highest mode observed for samples from the central Derryville Zone. Excluding the low salinity

369   population, the groups define points along a trend of decreasing temperature and increasing salinity,

370   similar to the data from Silvermines and Tynagh. Secondary, low T$_h$ brine inclusions were commonly

371   recorded.

372   Results from ore-stage and late ore-stage gangue phases fill out this trend with a more continuous

373   data distribution. Measurements from a ferroan calcite-cemented "white matrix breccia" (drillhole

374   LK262-100 m) from the Derryville Zone overlap most closely those from sphalerite. Rare data from

375   quartz fall at the more saline end of the distribution. Data from post ore-stage pink dolomite (D$_5$) and

376   secondary inclusions in calcite veins (and in sphalerite) fall at the end of this array indicating the late-

377   stage infiltration of low temperature brines into the deposit. Although these brines appear to

378   represent a viable end-member for the suggested mixing process (Eyre, 1998; Wilkinson et al.,

379   2005b), the pink dolomite itself is thought to significantly postdate mineralization and is related to

380   extensive sulfide dissolution. Thus it is inferred that multiple brine types infiltrated the deposit

381   during and subsequent to mineralization.

382   *Galmoy:* Fewer results are available from Galmoy but these show broadly similar characteristics to

383   Lisheen (Table 1). Sphalerite data display several salinity clusters in the range 10.8-16.3 wt% NaCl

384 equivalent and a relatively narrow range of homogenization temperatures between 129-179 °C

385 (Table 1), notably lower than at Lisheen. Hydrate melting was recorded in one sample at -22.4 ±0.2 °C

386 indicating predominance of NaCl over $CaCl_2$. Low T_h secondary inclusions were again common but no

387 salinity data are available. The sphalerite data overlap significantly with results from white matrix

388 breccia dolomite (D_3; see Fig. 2), consistent with a syn- ore-stage timing for these breccias as inferred

389 at Lisheen (Wilkinson et al., 2005b). Limited measurements on late ore-stage dolomite and calcite

390 yielded a wide range in T_h (111-228 °C) and salinity but are consistent with the possible mixing trend

391 defined at Lisheen.

392

393 *Subeconomic Prospects*

394 Studies of the subeconomic prospects in the orefield have been important in order to constrain

395 relative timing of mineralization in less intensely altered environments and to compare geological

396 characteristics with the larger systems to evaluate controls of economic mineralization. However, no

397 systematic comparison of the characteristics of the fluids involved has been carried out.

398 *Keel:* The Keel prospect and the adjacent Garrycam barite deposit (Fig. 1) have been widely

399 studied but never in great detail. The Keel deposit comprises stratabound breccia and fracture-fill

400 mineralization, localized by faults, that is hosted in rocks extending from the uppermost Silurian

401 basement slates up to the top of the Navan Group "Mixed Beds" (Slowey, 1986). It is distinctive in

402 that much of the sulfides occur as relatively coarse, euhedral crystals cementing breccias.

403 Subsequent to the initial study by Roedder, both Probert (1983) and Thompson (1992; cited in

404 Slowey et al., 1995) obtained T_h values in the range 110-187 °C and salinities of 11-24 wt% NaCl

405 equivalent but without detailed paragenetic control. Higher T_h values from barite at Garrycam were

406 considered to be unreliable. Later work reported data within this same range (Caulfield et al., 1986),

407 confirmed in this study on primary inclusions hosted by color-zoned sphalerite (Table 1). Late, pale-

408 yellow and transparent sphalerite trapped the coolest and lowest salinity fluids, interpreted to reflect

409 dilution of earlier, more saline and Fe-rich fluids. This pattern is similar to that recognized in

410 carbonate-base metal-gold epithermal deposits (Corbett, 2004). Post-sphalerite quartz contains the

411 most dilute inclusions (4.4-9.1 wt% NaCl equivalent; Collins, unpublished MSci dissertation, Imperial

412 College London, 2005; This study) suggesting that dilution eventually quenched ore formation. The

413 polymodal salinities observed at Keel-Garrycam, lack of evidence for mixing (with the exception of

414 the late dilution noted above), and range in T_h values suggest a complex history involving injection

415 and cooling of a number of fluid pulses.

416 *Harberton Bridge:* Harberton Bridge, located in Co. Kildare in the eastern part of the Midlands

417 (Fig. 1), is one of a number of small sulfide- and carbonate-cemented breccia deposits of Mississippi

418 Valley-type (Holdstock, 1982). The Kildare District has been widely cited as hosting an end-member

419 of the spectrum of styles of deposit in the orefield (Andrew, 1993; Wilkinson, 2003). Marcasite and

420 sphalerite are the dominant (commonly interbanded) sulfides with minor amounts of galena that

421 sometimes shows a recrystallized dendritic form (Trude and Wilkinson, 2001). The typical

422 paragenesis is early marcasite-calcite, often replacing or overgrowing limestone host rock, followed

423 by polymetallic marcasite-sphalerite-galena-calcite mineralization overprinted by late calcite

424 (Holdstock, 1982, 1983). Dolomite and pyrite are uncommon. This sequence is similar to that

425 described for the other Kildare deposits by Dixon (1990).

426 Preliminary T_h measurements of ~100 °C from Harberton Bridge were reported in a personal

427 communication by Finlow-Bates, cited in Emo (1986). The only systematic study, on representative

428 samples from one drillhole, found that monophase primary and secondary inclusions were abundant

429 in calcite, although two-phase inclusions of probable primary origin were also present (Trude and

430 Wilkinson, 2001). These yielded T_h values of 48-70 °C with an average of 61.5 °C, interpreted to

431 represent the upper end of the range likely for the calcite studied and indicating a very low

432 temperature origin for this style of mineralization. Hydrate melting was sometimes observed, ranging

433 from -37.2 to -21.8 °C, suggesting variable Ca:Na ratios. Salinities varied from 10.1 to 19.3 wt% NaCl

434 equivalent, possibly indicative of mixing.

435 *Kinnitty:* The Kinnitty prospect, located on the northwestern flank of the Slieve Bloom inlier (Fig.

436 1), is hosted by undolomitized Waulsortian Limestone and comprises stratabound calcite veins,

437 calcite-cemented breccias, and cavity infillings. Iron sulfides are dominant, mainly layered marcasite-

438 pyrite and melnikovite, and are typically interbanded with colloform sphalerite that contains galena,

439 sometimes with dendritic habit. A later overprint of calcite-pyrite veins and breccia is also observed.

440 Calcite associated with sphalerite-galena-marcasite assemblages hosts two-phase inclusions with

441 T_h values of 45-80 °C and modal salinity of 20-21 wt% with a total range of 8-22 wt% NaCl equivalent

442 (Table 1). Hydrate was commonly observed with a modal melting temperature of -21.3 °C indicating

443 dominance of Na over Ca (Strongman, unpublished MSci Dissertation, Imperial College London,

444 2001). The partial preservation of melnikovite, which converts to pyrite above 75 °C (Lepp, 1957), is

445 consistent with the very low temperatures. The spread in salinity suggests mineralization could have

446 been driven by mixing between a moderate salinity fluid (~14 wt%) and a more predominant brine

447 (~21 wt%). Variable mixing proportions could account for the strongly oscillating chemistry and pH

448 implied by the multiple interbanding of calcite(-melnikovite/pyrite) and marcasite.

449 *Cooleen:* The Cooleen Zone is a satellite of the Silvermines system (Lee and Wilkinson, 2002) that

450 was explored by Ennex International in the 1990's before being abandoned as uneconomic.

451 Mineralization is replacive and is focused within partially and wholly dolomitized sedimentary

452 breccias. It comprises stratiform massive, semi-massive and disseminated sulfides dominated by

453 pyrite with lesser sphalerite and minor galena. Galena is intimately associated with sphalerite,

454 sometimes forming bands of cubic crystals or dendrites located within and often at the core of

455 growths of colloform sphalerite. Mineralized calcite and dolomite veins underlie and crosscut

456 massive sulfides.

457   Fluid inclusion data were obtained from late ore-stage dolomite and calcite veins that cut massive

458 sulfide mineralization and which have walls intermittently lined by euhedral, pale brown to orange-

459 brown sphalerite and galena (Lee, 2002). Inclusions were usually two-phase liquid-vapor type,

460 although monophase inclusions were also observed in the calcite veins. A clear distinction was noted

461 between inclusions hosted by dolomite (modal T_h = 180-190 °C; salinity = 10.8-17.6 wt% NaCl

462 equivalent) and calcite (modal T_h = 150-160 °C; 4.8-14.2 wt% NaCl equivalent) with the former data

463 showing a cluster and the latter displaying a trend from this cluster toward lower T_h and salinity

464 values, interpreted to represent dilution. The few sphalerite-hosted inclusions measured fell into two

465 groups: vein-hosted sphalerite contained inclusions comparable to those hosted by dolomite

466 whereas a fragment of sphalerite interpreted to be a reworked clast in a sedimentary breccia hosted

467 inclusions with much lower T_h and salinity values (Table 1).

468   *Rathdowney Trend:* In the Rathdowney Trend (Fig. 1), prospects at Holycross, Durrow and

469 Rathdowney East were sampled for reconnaissance studies by Eyre (1998). A variety of

470 mineralization styles are observed, principally disseminated, replacement and fracture-fillings

471 associated with hydrothermal black (D_2) and white (D_3) dolomite.

472   Sphalerite- and vein dolomite-hosted inclusions from Holycross display a prominent mode in T_h at

473 170-180 °C with salinity modes at 10-11 and 16-17 wt% NaCl equivalent (Table 1), very similar to

474 Lisheen. Hydrate melting was observed at -22.7 °C, identical to Lisheen and Galmoy sphalerites

475 (Table 1). Relatively high and variable homogenization temperatures of 155-267 °C (principal mode

476 210-220 °C) were recorded for primary inclusions hosted by coarse white dolomite-cemented

477 breccias. On average, these inclusions display higher T_h and slightly lower salinity than sphalerite-

478 hosted inclusions in the Rathdowney Trend deposits or prospects and could represent high-

479 temperature, end-member ore fluids prior to fluid mixing. Pink dolomite (D_5) in the Rathdowney

480 Trend contains similar inclusions to those observed in the same phase at Lisheen and Galmoy but

481 with a slightly higher modal T_h range (110-120 °C compared with 90-100 °C and 80-90 °C

482 respectively). Secondary, low T_h brine inclusions (28-29 wt% NaCl equivalent), similar to those in pink

483 dolomite, are common in the Rathdowney Trend prospects.

484   *Courtbrown:* The Courtbrown prospect is located in the southwest Midlands, west of Limerick (Fig.

485 1). Mineralization occurs as replacement and disseminated styles and is commonly associated with

486 solution seams (Grennan, 1986). Two-phase fluid inclusions in ore-stage calcite yielded T_h values

487 mainly in the range 160-190 °C (Reed and Wallace, 2001). Freezing data were not reported. Although

488 these results are within the most common range for fluids in the orefield (Table 1), no petrographic

489   evidence for stretching was described, and no size-T_h relationship exists, the authors concluded that

490   the inclusions must have undergone post-entrapment modification based on inferred overheating to

491   ~310 °C (Reed and Wallace, 2001).

492   *Pallas Green:* The Pallas Green prospecting licences are located in the southwest Midlands (Fig. 1).

493   Five massive sulfide lenses have been discovered in the area: two small zones at Castlegarde and

494   three larger lenses at Tobermalug, Caherconlish South and Srahane West. This area is currently

495   undergoing intense exploration and is arguably the most prospective greenfield region in the

496   orefield. Mineralization at Castlegarde comprises a variety of replacement, breccia and cavity-fill

497   styles. Early marcasite and pyrite, which may form massive intervals in drillcore, partly replace early

498   calcite cements and Waulsortian hostrock clasts. Sphalerite is often very finely color-banded, partly

499   replaces earlier Fe sulfides, and contains later euhedral and dendritic galena (Crowther and

500   Wilkinson, unpublished report to the Noranda-Minco joint venture, 2002).

501   Two-phase fluid inclusions were analyzed in calcite that infills sulfide-lined vugs and is sometimes

502   replaced by sulfides. The majority of T_h values ranged from 132-181 °C with a mode of 150-160 °C.

503   Salinities varied from 16.1 to 4.3 wt% NaCl at approximately constant T_h possibly indicative of a

504   dilution trend.

505

506   *Regional Carbonate Cements*

507   Fluid inclusion studies on cement phases within the Lower Carboniferous host rock sequence

508   began in the early 1990's. However, a clear picture of the relationship between cementation stages

509   and hydrothermal events did not begin to emerge until more detailed fluid inclusion studies were

510   carried out on exploration drillcore through the late 1990's (Wilkinson, unpublished data, 1996-2000)

511   and a regional study of the Lower Carboniferous cements and their associated fluid inclusion

512   populations was begun (Gregg et al., 2001; Johnson et al., 2001, 2009).

513   *Fine replacive dolomite (D_{1a}):* Reliable fluid inclusion data have not been obtained from the early

514   (pre-ore) diagenetic planar dolomite (Fig. 2) due to its fine grain size. Based on textural and isotopic

515   constraints, this has been interpreted as an early, seawater-related diagenetic product (Gregg et al.,

516   2001).

517   *Coarse white dolomite (D_{1b}):* A few T_h data were reported from aqueous liquid-vapour inclusions

518   in coarse white "regional" dolomite (Fig. 2) in the 1990's (Allan et al., 1992; Eyre, 1998) suggesting

519   precipitation temperatures up to 233 °C and apparently ruling out a simple diagenetic origin (cf.

520   Hitzman, 1995; Hitzman et al., 1998). Subsequent work on similar, non-planar replacement dolomite

521   yielded rare data from two-phase aqueous inclusions with T_h values of 170-200 °C and salinities of

522   ~2-15 wt% NaCl equivalent (fluid "Type 2": Gregg et al., 2001). It was concluded that this cement

523   probably originated via partial neomorphic recrystallization and overgrowth of the early planar

524 dolomite in the presence of late diagenetic or hydrothermal fluids. More recent studies have

525 reported the common occurrence of aqueous liquid-vapour fluid inclusions, distributed along growth

526 zones, in Waulsortian-hosted samples of coarse white dolomite from throughout the Midlands

527 (Wilkinson, unpublished data; Wilkinson, 2003). T_h data are in the range 140-240 °C with salinities of

528 10-15 wt% NaCl equivalent, identical to the majority of hydrothermal fluids observed in the deposits

529 (Table 1).

530   *White dolomite-cemented breccias:* Breccias cemented by planar to non-planar white dolomite

531 (Fig. 2) are similar to the white matrix breccias associated with mineralization (Doyle et al., 1992;

532 Hitzman et al., 2002; Wilkinson et al., 2005b) in terms of texture, cathodoluminescence and primary

533 liquid-vapor fluid inclusion properties (Wilkinson, 2003; Table 1). These inclusions have similar

534 salinities but slightly higher T_h values than those hosted by coarse white dolomite and some develop

535 clathrate on cooling, indicative of elevated CO_2, as previously reported from deposit sphalerite and

536 Lower Paleozoic-hosted quartz-carbonate veins (Everett et al., 1999a).

537   An unusual dolomite with uncertain paragenetic position has also been studied. This generally

538 comprises fine- to coarse-grained, planar-subhedral turbid crystals that commonly display a

539 pearlescent appearance and cream to pinkish color in hand sample. It appears to be replacive in

540 origin and is texturally similar to the fine replacive regional dolomite (Fig. 2) except for its coarser

541 grain size. It is often overgrown by translucent dolomite, occasionally with red or brown ferroan

542 growth bands, that displays weak, non-planar form (Fig. 4B). Late, transparent vug-filling calcite may

543 be present, possibly equivalent to C_6 (Fig. 2). Primary inclusions in growth bands are common in the

544 translucent dolomite and these have similar properties to those observed within some of the earlier

545 turbid dolomite; therefore, they are both thought to have precipitated from the same fluid type.

546 Average first melting temperatures of -53.2 °C indicate the predominance of NaCl and $CaCl_2$. Final ice

547 melting temperatures are unusually low, ranging from -23.0 to -35.3 °C (Fig. 4B) and, where

548 observed, hydrohalite melting occurs after ice with a mean temperature of -1.7 °C (Table 1). These

549 data imply distinctive Ca-rich brine compositions.

550   *Black dolomite:* Breccia samples from Ballinasloe in the west-central Midlands (Fig. 1) yielded the

551 only fluid inclusion data yet to be acquired from fine planar black dolomite of the type elsewhere

552 associated with ore in the Waulsortian-hosted deposits (Wilkinson and Earls, 2000; Fig. 2). This

553 yielded T_h values of 146-204 °C, salinities of 13.5-19.9 wt% NaCl equivalent and $T_m$hyd in a few

554 inclusions close to -22 °C indicating NaCl-dominant compositions comparable with inferred ore-stage

555 fluids at Silvermines, Tynagh, Lisheen and Galmoy. The spread in salinity was considered to be due to

556 mixing of a moderate salinity (~12 wt%), higher temperature fluid with a low temperature brine; this

557 process induced rapid supersaturation and precipitation of the characteristic dolomite type. Slightly

558 earlier white to translucent dolomite that formed reaction rims around breccia clasts hosted two-

559   phase inclusions with T_h values of 144-203 °C and salinities of 10.3-13.5 wt% NaCl equivalent, similar

560   to coarse white dolomite elsewhere.

561   *Pink dolomite:* Paragenetically late, coarse grained, cream to pink dolomite (Fig. 2), is widely

562   observed in the Midlands as a replacement, vug- and vein-filling cement phase (e.g., Boast et al.

563   1981; Andrew 1986; Eyre 1998), and has also been described cutting mineralized veins in the Lower

564   Paleozoic basement (Everett et al., 1999a). It displays a well-developed saddle morphology and

565   shows pronounced compositional zoning in CL (Wilkinson, 2003). It commonly occurs as an

566   overgrowth of earlier coarse white dolomite in vugs and, as a result, may be confused with this

567   earlier dolomite. Minor sulfides (mainly pyrite, chalcopyrite and sphalerite) are occasionally observed

568   encrusting pink dolomite crystals which may explain why this dolomite has been interpreted as pre-

569   ore (Wright et al., 2000). However, where observed in the deposits, it is always post-ore and is

570   associated with extensive dissolution of sulfides (Boast et al., 1981; Eyre, 1998).

571   The pink dolomite contains two-phase liquid-vapour inclusions with very consistent properties

572   (Table 1). Homogenization temperatures are mostly in the range 91-137 °C and salinities are 23.7-

573   24.7 wt% NaCl equivalent. First melting is normally observed below -50 °C indicating significant $CaCl_2$,

574   but combined ice and hydrate melting temperatures (average -17.9 °C) indicate that these brines

575   have Na>Ca.

576   *Other dolomite data:* Gregg et al. (2001), Mulhall (2003) and Johnson et al. (2001, 2009) identified

577   three main types of fluid in the Midlands based on inclusions hosted by "late diagenetic" saddle

578   dolomite cements, but the relative timing of the hosting dolomites was not fully resolved. Based on

579   analogy with known fluids elsewhere in the Midlands it is considered probable that the saddle

580   dolomite that hosts inclusions homogenizing in the range 100-270 °C and with salinities of 0-17 wt%

581   NaCl equivalent ("Type 2" and "Type 3" fluids: Gregg et al., 2001) is correlatable with coarse white

582   and/or white matrix breccia dolomite (Fig. 2), whereas the white to pink saddle dolomite cements

583   hosting inclusions with T_h values of 70-120 °C and salinities of 19 to >26 wt% NaCl equivalent are

584   likely to be equivalent to the late (post-ore) pink dolomite described above. The difficulty in

585   distinguishing between some of the dolomite types is probably due in part to the development of

586   epitaxial overgrowths. For the late pink dolomite, its field distinction is largely based on a coloration

587   that is not always developed. Significantly, the "Type 3" fluid, that has comparable properties to the

588   ore-forming fluids (Table 1), was not observed in Supra-Waulsortian lithologies (Johnson et al., 2001,

589   2009), consistent with a principal high-temperature hydrothermal event that predated their

590   deposition (e.g., Lee and Wilkinson, 2002).

591

592   *Footwall stratigraphy*

593   The first study of fluid flow at greater paleodepths investigated the structural, mineralogical and

594   isotopic characteristics of vein systems hosted by Lower Paleozoic rocks. This was coupled with fluid

595   inclusion data to test whether mineralizing fluids had circulated in fracture permeability within this

596   volcanosedimentary succession (Everett et al., 1999a). Three main vein types were identified that cut

597   dark grey-green Silurian greywackes, mudstones and sandstones in the southwest Irish Midlands at

598   locations up to 32 km WSW and 20 km ESE of Silvermines (Fig. 1):

599

600   1. Early hematitic calcite-quartz ± pyrite

601   2. Quartz-calcite ± sphalerite, galena, chalcopyrite, pyrite, barite

602   3. Ankerite-ferroan dolomite-quartz ± sphalerite, pyrite

603

604   Vein types 2 and 3 are associated with weak to locally intense sericite-chlorite-carbonate alteration,

605   and disseminated pyrite(-carbonate) is observed in the vicinity of well-developed vein systems. Clots

606   of a distinctive fine-grained pistachio green mineral are commonly observed within Type 2 veins and

607   along vein margins and more rarely in Type 3 veins. In some cases it is associated with pink dolomite

608   that cuts both vein types. Microprobe analyses indicate that these comprise phengitic K-mica,

609   sometimes intimately intergrown with chlorite.

610   The majority of the fluid inclusions observed were of liquid-vapor aqueous type with a minority of

611   secondary monophase, liquid-only inclusions. Inclusions within quartz which showed a highly variable

612   degree of fill from 5 to 75 percent liquid were recorded in one sample – possible evidence for boiling.

613   Some liquid-vapor and liquid-only inclusions contained trapped solid phases that showed no change

614   upon heating; these were interpreted to be calcite and K-mica.

615   Inclusions considered to represent the vein-forming fluids in Type 1 veins had low to moderate

616   salinities (0.2-10.8 wt% NaCl equivalent) and T_h values from 150-250 °C. Lower temperature (109-

617   189.9 °C), moderate to high salinity (12.2-23.8) secondary inclusions were also recorded. The origin

618   of the Type 1 veins is uncertain, although structural relationships are consistent with a Lower

619   Carboniferous age, and the occurrence of hematite, chlorite and calcite is similar to the early (pre-

620   sulfide) ironstones and associated hematite-bearing veins reported at several Irish base metal

621   deposits (Hitzman et al., 1995). However, the fluid properties are also comparable with inclusions

622   commonly associated with the Caledonian granites in Ireland, interpreted to represent widespread

623   meteoric circulation subsequent to their emplacement and crystallization (O'Reilly et al., 1997a,b).

624   Primary fluid inclusion data from vein Types 2 and 3 show T_h-salinity characteristics (123-238 °C,

625   9.7-20.6 wt% NaCl equivalent) that are comparable with data from Carboniferous-hosted

626   mineralization (Table 1). In addition, the highest T_h inclusions hosted by quartz and sphalerite

627   commonly contain CO_2 as noted elsewhere. These fluids are believed to represent ore fluids trapped

628   en route to potential sites of mineralization.

629

630   **Fluid Inclusion Constraints on Fluid Origins and Interactions**

631

632   Although basic microthermometric data provide important constraints on fluid properties and

633   variability within hydrothermal ore systems (e.g. Wilkinson, 2001), greater insights are provided by

634   more complete fluid geochemical information. At the first level, this includes interpretation of ice

635   and hydrate melting temperatures in the $NaCl$-$CaCl_2$-H_2O system which yields information on trends

636   in the major cation compositions of the fluids. More detailed geochemical studies, using bulk

637   methods (crush-leach or decrepitation-linked ICP analysis), have also been carried out in Ireland,

638   principally to provide constraints on the origin of the ore-forming solutions. The use of laser ablation

639   ICP-MS for the analysis of individual inclusions is just starting to be applied and is providing

640   important new data on metal contents (Wilkinson et al., 2009).

641

642   *Na:Ca ratios*

643   In order to interpret fluid inclusion chemistry in chemical systems more complex than $NaCl$-H_2O

644   from microthermometric data it is necessary to observe additional phase changes, such as hydrate

645   melting. However, in studies of the Irish orefield this phase transition has been reported only rarely

646   (Samson and Russell, 1987; Banks and Russell, 1992; Eyre, 1998). These results indicated that fluids

647   generally had Na numbers (Na#: $NaCl$/[$NaCl$+$CaCl_2$]) greater than 0.5. Based on crush-leach data,

648   Samson and Russell (1987) suggested that the moderate salinity ore fluids had high Na# and that two

649   brine types existed, one with high Na# and one with low Na#.

650   Here, new data are presented from basement-hosted veins, regional carbonates, deposits

651   (Silvermines) and prospects (Keel and Castlegarde). Excluding three outliers below -30 °C (probably

652   erroneous observation), T_mhyd ranges from to -29.0°C to +1.1 °C, but is mostly between -22 and -24

653   °C (Table 1). Modelling ice and hydrate melting in the $NaCl$-$CaCl_2$-H_2O system (Naden, 1996) gives

654   Na# mostly in the range of 0.66-0.95 for basement-hosted veins, 0.42-0.88 for regional carbonates,

655   and 0.61-0.92 for deposits and prospects. The uncertainty for careful measurement of T_mhyd is ±0.2

656   °C and for ice melting ±0.1 °C which translates into a modeled uncertainty of +0.03/-0.01 in Na# and

657   ±0.1 wt% in total salinity (wt% $NaCl$+$CaCl_2$ equivalent). The degree of uncertainty due to the presence

658   of other cations or anions in the fluids cannot be assessed. Plotting Na# as a function of total salinity

659   allows possible end-member fluids and mixing relationships to be identified (Fig. 5).

660   The regional carbonate data suggest that two brine compositions exist with Na# of ~0.75 (25 wt%

661   salinity; Type B_1) and Na# ~0.60 (28 wt% salinity; Type B_2), in agreement with Samson and Russell

662   (1987). Type B_1 is principally associated with pink dolomite and has compositions similar to Triassic,

663   red-bed derived, evaporitic brines recorded in Southwest England (Gleeson et al., 2001; Stoffell et al.,

664   2004). It corresponds to the "Group 3" calcite-hosted inclusions of Banks and Russell (1992) at

665   Tynagh. Type B_2 is associated with cream to pink, turbid, replacement dolomite or the more

666   transparent dolomite that overgrows it. A third, calcic brine (B_3), sometimes spatially associated with

667   the B_2 brines (Fig. 4), is inferred from inclusions that display very low ice melting temperatures

668   (typically around -33 °C). Although hydrate melting generally was not observed, the topology of the

669    $NaCl$-$CaCl_2$-H_2O phase diagram indicates variably Ca-rich fluid compositions with Na# between ~0.2

670   and 0.6. These fluids have been found associated with Supra-Waulsortian dolomitized shelf

671   limestones to the west of Ballinasloe and younger (up to Holkerian or early Asbian) shelf limestones

672   southwest of Stradbally in Co. Laois (Fig. 1) indicating that they were present (although not

673   necessarily exclusively) post-mineralization.

674   Results for moderate salinity fluids in basement-hosted veins (LP_1) indicate relatively high Na#

675   (0.7-0.9), typical for ore fluids from Silvermines (Samson and Russell, 1987). Basement-hosted

676   sphalerite typically displays average Na# ~0.75 at the lower end of this range. The variation in Na# as

677   a function of total salinity could reflect LP_1-B_2 mixing in the upper parts of the basement immediately

678   beneath the basinal succession or salinity-dependent siliciclastic buffering of fluid composition, with

679   lower Na/Ca characterizing slightly higher salinity fluids (e.g., Yardley, 2005). However, there are

680   insufficient data to properly constrain these possibilities at present.

681   Deposit-hosted sphalerite trapped fluids of distinct composition that are of relatively low salinity

682   but more calcic than the LP_1 fluids. It is therefore possible that the actual ore-forming fluids were of

683   somewhat different composition (particularly in their metal budget) to at least some of the fluids

684   trapped in feeder veins in the basement as has recently been suggested on the basis of LA-ICP-MS

685   analyses of inclusions (Wilkinson et al., 2009). The more calcic compositions could be indicative of

686   greater degrees of fluid-rock interaction (see below). Alternatively, it may be that fluid compositions

687   were shifted toward more calcic compositions during ore deposition. Sphalerite precipitation as a

688   result of fluid mixing generates acid that can result in carbonate dissolution and consequent Ca

689   (+Mg) enrichment in the fluid according to reactions such as:

690

691            $2\ ZnCl_4^{2-} + 2\ H_2S + CaMg(CO_3)_2 = 2\ ZnS + 8\ Cl^- + Ca^{2+} + Mg^{2+} + 2\ H_2CO_3$

692

693   This type of reaction is supported by abundant textural evidence for delicate replacement of

694   different carbonate grain types by sulfides, as has been described from Lisheen (Wilkinson et al.,

695   2005b). A third possibility is that ore formation resulted from mixing between fluids of LP_1 type and

696   the calcic B_3 brines (Fig. 5). However, this is thought to be unlikely given the young (probably post-

697   ore) age of the B_3 brines identified to date.

698

699   *Major element chemistry*

700   Bulk fluid inclusion analyses on quartz from basement-hosted vein samples (Everett et al., 1999a)

701   showed that LP_1 fluids had Na>Ca≥K and were Mg-poor. These compositions are comparable with

702   experimental data on fluids equilibrated with greywackes at temperatures of 200-350 °C, consistent

703   with derivation of mineralizing fluids from a Lower Paleozoic-equilibrated fluid reservoir. Na# were in

704   the range 0.88-0.94, consistent with the microthermometry-derived values reported here. Na-K-Ca

705   (Fournier & Truesdell, 1973) and K-Na and K-Mg alkali thermometers (Giggenbach, 1988) can be

706   applied because the mineralogy of the Lower Paleozoic succession (quartz, albite, K-feldspar,

707   muscovite, chlorite, illite, minor carbonate, trace sulfides) is similar to that in the geothermal

708   reservoirs from which the thermometers are calibrated. These geothermometers gave equilibration

709   temperatures (158-219 °C) not significantly different to T_h values suggesting that the inclusions were

710   trapped under pressures only slightly above saturated vapor pressure, indicating a relatively shallow

711   depth of vein formation. In terms of the detail of flow patterns and the relationship between these

712   feeder vein localities and the deposits, it may be important that these temperatures are lower than

713   many of the estimates for fluid temperatures in the ore deposits (Table 1).

714

715   *Halogen geochemistry*

716   The first halogen analyses of Irish fluids were presented by Everett (1999), Everett et al. (1999b)

717   and Gleeson et al. (1999), and were further expanded by Banks et al. (2002), Wilkinson et al. (2005a)

718   and Johnson et al. (2009). Although the uncertainty in these measurements is difficult to constrain,

719   different fluid types can be identified based on significant differences in halogen and major element

720   ratios and/or the restriction of particular signatures to specific paragenetic stages or geographic

721   locations.

722   Lower Paleozoic-hosted vein samples contain fluids that fall into two groups: Type LP_{1a} have Cl/Br

723   molar ratios (559-825) that are similar to seawater, interpreted as being produced by partial

724   evaporation of seawater to an evaporation ratio of ~4x to ~7x (evaporation ratio = mass of water in

725   seawater/mass of water in evaporated brine) prior to circulation into the basement (Wilkinson et al.,

726   2005a). Type LP_{1b} fluids are slightly less saline but have Cl/Br values below seawater (375-553); these

727   were interpreted to represent strongly evaporated bitterns (evaporation ratio up to 25x), relatively

728   enriched in Br, that had subsequently been diluted by either seawater, evaporated seawater or

729   meteoric water (Fig. 6A). Mixing curves show that the data are consistent with mixtures containing

730   ~5-20% brine (by mass) and ~80-95% evaporated seawater although other possibilities cannot be

731 excluded at present. The relatively narrow salinity range displayed by the LP_{1b} fluids (Everett et al.,

732 1999a) implies homogenization of these putative mixtures prior to trapping but it is uncertain when

733 this mixing occurred: prior to recharge, during flow within basement rocks, or close to the

734 paleosurface around the time of mineralization. Hydrogen and oxygen isotope data (see below) are

735 consistent with a model involving mixing of uninteracted brines (relatively near to the paleosurface)

736 with strongly interacted LP_1-type fluids to form the LP_{1b} fluids.

737   Results from deposit-hosted samples show that ore fluids from Silvermines are similar to LP_{1a}

738 whereas those from Tynagh are shifted to slightly more Br-rich compositions, closer to LP_{1b}. Tentative

739 modeling indicates that mixing between Br-enriched brines (<20%) and LP_1 fluids (evolved partially

740 evaporated seawater; >80%) can produce most of the range in Cl-Br compositions observed in the

741 Irish ore fluids (Fig. 6A) although it is possible that some of the spread is an artefact due to analysis of

742 inhomogeneous inclusion populations. Nonetheless, the data are consistent with trapping of

743 mixtures of high temperature fluids and brines at the ore depositional site, a process that has been

744 invoked as a key ore-forming mechanism (e.g. Anderson et al., 1998; Blakeman et al., 2002; Hitzman

745 et al., 2003; Wilkinson et al., 2005a, 2005b).

746   Combining exchangeable cation data with the conservative halogens allows processes undergone

747 by these seawater-derived fluids during crustal interaction to be explored. A plot of Cl/Br vs. Na/Br

748 (Fig. 6B) shows that all deposit and Lower Paleozoic basement-hosted vein data lie close to or above

749 the seawater evaporation trajectory (SET), best explained by loss of Na from fluids initially lying at

750 various points along the SET. Fluids from Silvermines appear to be more exchanged than those from

751 Tynagh, possibly accounted for by a greater degree of water-rock interaction, which could explain

752 the greater metal endowment of the Silvermines system. Both deposits appear to have formed from

753 more exchanged fluids (subsequently referred to as LP_2) than the Lower Paleozoic-hosted veins,

754 suggesting that the feeder veins (sampled lateral to the deposits) represent different, less basement-

755 interacted, parts of the flow system. The samples from Birdhill and Latteragh (closer to Silvermines;

756 Fig. 1) generally display greater degrees of Na loss than those from Fantane and Ballycar (Fig. 6B),

757 consistent with a convective type of flow pattern.

758   An equivalent plot but involving Ca (Fig. 6C) shows that there is very strong enrichment in Ca in

759 the Lower Paleozoic-hosted vein fluids relative to evaporated seawater. Unfortunately, no

760 comparable data for deposit-hosted inclusions exist. The exchange of Ca^{2+} for $2Na^+$, most commonly

761 mediated by reactions involving plagioclase, is a common process in crustal fluid-rock interactions

762 and is related to temperature and fluid salinity (Yardley, 2005). Ca is most enriched in samples from

763 the Birdhill and Latteragh localities supporting greater degrees of exchange in the genesis of these

764 fluids, consistent with the Na data. However, consideration of the cation balance shows that the Ca

765 gain in the LP_1 fluids is not matched by twice as great a loss (in molar terms) in Na so that an

766 additional source of Ca is required. One possibility is that Ca was acquired from the Carboniferous

767 sequence as a result of Mg-Ca exchange dolomitization in downflow zones:

768

769 $$2CaCO_3 + Mg^{2+} = CaMg(CO_3)_2 + Ca^{2+}$$

770

771 Some of the pre-mineralization, seawater-related dolomitization observed (D_{1a}) could have been

772 formed in this way and the process may also have been responsible for some of the Mg depletion

773 noted in the LP_1 fluids, although this can also be attributed to Mg-smectite and chlorite formation in

774 the basement rocks (see below).

775 Microthermometric data suggest that deposit sphalerite-hosted ore fluids (LP_2) are even more Ca-

776 rich than LP_1 fluids (Fig. 5) and this is supported by recent LA-ICP-MS analyses (Wilkinson et al.,

777 2009). This is consistent with greater degrees of basement exchange in their production although, as

778 noted earlier, the possibility of local Ca increase due to carbonate dissolution at the site of ore

779 formation cannot be excluded.

780

781 *Minor and trace element chemistry*

782 Plotting the minor and trace element chemistry of the LP_1 fluids normalized to their inferred

783 evaporated seawater precursor illustrates the Li enrichment, strong Mg depletion, and broad

784 increase in the transition metals and lithophile elements (Sr, Ba, Pb), that has occurred during crustal

785 interaction (Fig. 7). Similar changes are observed in modern seawater-dominated submarine

786 hydrothermal fluids interacting with ocean basalts, but with a lack of such strong enrichment in

787 elements concentrated in felsic crust such as Ba or Pb.

788 Lithium concentrations in LP_1 fluids are in the range 55-164 ppm (Everett et al., unpublished;

789 Wilkinson et al., 2005a), overlapping with, but generally lower than, the 86-503 ppm obtained by

790 crush-leach analysis from Silvermines and Tynagh ore-stage samples (Banks et al., 2002). All these

791 values are elevated significantly above evaporated seawater concentrations. Enrichment is most

792 likely due to interaction with basement rocks that typically contain 30-60 ppm Li (Crowther, 2007).

793 Magnesium concentrations in LP_1 fluids are in the range 30-310 ppm and are very depleted (Fig.

794 7), typical of seawater-derived fluids that have undergone low temperature exchange with silicate

795 rocks and/or have been involved in dolomitization. Thus, the Mg data, like Na, can be explained by

796 exchange for Ca during fluid infiltration.

797 Barium is strongly enriched in LP_1 fluids, such as at Fantane (mean 930 ppm; Wilkinson et al.,

798 2005a), even in the absence of significant base metals. It could be acquired by fluids from trace

799 barite or barian feldspar during basement interaction, but only once fluids were depleted in sulfate

800 either by anhydrite precipitation or reduction.

801   Bulk data suggest that ore metal concentrations are low in LP_1 fluids (2-33 ppm Zn, 11-68 ppm Pb;

802   Everett et al., unpublished; Wilkinson et al., 2005a) and are highest in the most interacted fluids

803   (based on Na/Br systematics) at Birdhill and Latteragh. This contrasts markedly with recent analyses

804   of sphalerite-hosted inclusions from Silvermines that display one to two orders of magnitude higher

805   Pb concentrations (Wilkinson et al., 2009). Such high metal contents appear to suggest that unusually

806   efficient metal extraction was responsible for production of the LP_2 fluids that went on to form ore,

807   potentially linked to the greater degrees of water-rock interaction suggested above.

808

809   *Oxygen and hydrogen isotopes*

810   Fluid δD (obtained by direct measurement of fluid inclusions) and calculated fluid $\delta^{18}O$ values

811   (based on mineral compositions and mineral-water fractionation factors) from ore-stage samples at

812   Silvermines were interpreted to reflect equilibration of seawater-derived fluids with the Lower

813   Paleozoic sequence (Samson and Russell, 1987). Similar data from Lower Paleozoic-hosted feeder

814   veins (Everett et al., 1999b) suggested mineralizing solutions with $\delta^{18}O_{H2O}$= 2.4-9.0‰ and δD= -24 to -

815   55‰, overlapping with the Silvermines orefluids. This is supporting evidence for Lower Paleozoic

816   flow of the ore-forming solutions, although the generally lower δD of the Silvermines fluids is

817   noteworthy.

818   Modeling of these data using the new constraints on fluid origins discussed above shows that the

819   measured compositions cannot be produced by equilibration of seawater or evaporated seawater

820   with inferred Lower Paleozoic rock compositions, even at low water/rock ratios (Fig. 8). Utilising a

821   possibly depleted Carboniferous seawater precursor ($\delta^{18}O$ = -3‰; Veizer et al., 1999) has negligible

822   effect because fully-equilibrated fluids at low water/rock ratios are essentially buffered by the rock

823   composition. The discrepancy requires involvement of an unexchanged fluid with much lower δD,

824   lower fluid-rock fractionation factors for hydrogen and/or lower δD of the rocks involved. The

825   observation that low temperature brine inclusions trapped in barite at Silvermines are characterized

826   by low δD values (-41.4 to -54.6 ‰; Samson and Russell, 1987) suggests that a D-depleted shallow

827   brine may have existed and mixing between this and exchanged evaporated seawater could explain

828   the relatively D-depleted LP_1 fluid data and some of the ore fluid compositions (Fig. 8). A possible

829   explanation for the depleted brine signature is bacterial fractionation of hydrogen isotopes at the

830   seafloor (Samson and Russell, 1987); however, it can also be reproduced by shifting the seawater

831   evaporation trajectory to lower $\delta^{18}O$ and δD values and assuming a depleted Carboniferous seawater

832   precursor (Fig. 8). Thus, the low δD signature could be merely a product of evaporation past halite

833   precipitation (cf. Knauth and Beeunas, 1985).

834 The isotopic compositions of the bulk of the Silvermines ore fluids (which tend to have higher T_h

835 values and lower salinities than most LP_1 fluids) cannot be explained by brine-LP_1 mixing in the ore-

836 forming environment (Fig. 8) and appear to require a greater hydrogen isotope shift during fluid-rock

837 interaction. The involvement of D-depleted lithologies at greater depth cannot be tested although

838 this would be consistent with the higher fluid temperatures suggested by higher $\delta^{18}O$ values and

839 generally higher T_h values. Interaction with mafic rocks (δD -70 to -105 %; Agrinier et al., 1995),

840 Caledonian granite or the Precambrian crystalline basement that may have undergone earlier

841 deuteric alteration are all possibilities.

842

843   **Discussion and Implications**

844

845 *Regional fluid evolution*

846 Fluid inclusion data, coupled with stable and radiogenic isotope systematics, describe a basinal

847 system in which widespread mobilization of hydrothermal fluids led to progressive overprinting of

848 normal, early diagenetic processes and localized convergence of a number of factors toward ore-

849 forming conditions. Fluid chemistry suggests that some of the early dolomitization (D_{1a}; Fig. 2) could

850 have formed from "normal" evaporated seawater that subsequently penetrated the basement and

851 evolved into interacted but unfertile solutions. Regionally-developed, coarse white dolomite cements

852 (D_{1b}) then formed above fault-focused plumes of these evolved solutions, as they became thermally

853 buoyant and migrated back toward the surface. The coarse white dolomite is thus interpreted to

854 reflect a slightly lower temperature and spatially more extensive manifestation of the hydrothermal

855 system that was ultimately responsible for the formation of the ore deposits (Wilkinson, 2003).

856 Increased focusing and greater penetration depth are inferred to have led to the local generation

857 of higher temperature, more exchanged, highly metalliferous fluids. It was only where these LP_2

858 fluids returned to the near seafloor environment and mixed with sulfidic brines that economic

859 mineralization was formed, accompanied by hydrothermal dolomite (D_2, D_3). Continued flow of these

860 fluids after the main mineralizing event(s), with brines excluded from the ore systems perhaps by the

861 deposition of impermeable capping sequences (e.g., Calp Limestone over the Waulsortian; Upper

862 Dark Limestones over the Navan Group), led to overprinting of ore by late stage veins in some of the

863 deposits (D_4, C_4).

864 The late pink dolomite (D_5) is a distinct, post-ore marker that has been interpreted in terms of a

865 post-ore brine migration, probably related to the onset of Variscan compressional tectonism in the

866 mid- to late Carboniferous (Andrew, 1986; Wilkinson, 2003; Wilkinson et al., 2003). Thus, the onset

867 of compression in the Midlands Basin is considered to have been the principal tectonic control that

868 switched off convective fluid circulation.

869

Regional variations in fluid properties

The compilation of microthermometric data presented resolves some trends not previously recognized. Plotting principal modal T_h and salinity data from each locality (Fig. 9) shows that there is a regional pattern, with lower T_h and/or lower salinity fluids predominant in the north and western Midlands and higher T_h, higher salinity fluids in the south and east. This division corresponds broadly to the position of the Iapetus Suture Zone (Fig. 1) and it is proposed that this marks a major discontinuity between flow systems operating in the two halves of the Midlands Basin. Evidence for a contrast in the chemical composition of fluids in the northern Midlands compared with the south was previously suggested by Wilkinson et al. (2007) based on a preliminary regional LA-ICP-MS study of fluid inclusions in feeder veins. This showed that Zn:Pb ratios and Zn contents were significantly higher in the northern Midlands localities investigated, possibly related to a greater volcanic contribution in the Lower Paleozoic basement to the north of the Iapetus Suture. The generally lower T_h values in the northern domain is presumed to reflect a shallower circulation system, possibly limited by a thinner Lower Paleozoic sequence underlain by relatively impermeable Dalradian or Lewisian metamorphic rocks. Nonetheless, some interaction with the crystalline basement in the north has been suggested based on Nd isotope analyses of hydrothermal carbonates (Walshaw et al., 2006).

Higher temperatures, particularly in the southwest, are consistent with the lower Zn:Pb ratios in these fluids and higher $\delta^{18}O$ values. At Tynagh and Silvermines, there is evidence that submarine warm springs developed (Banks, 1985; Boyce et al., 2003; Wilkinson et al., 2003, 2005a) perhaps because these rising fluids were more buoyant due to their higher temperatures and lower salinities and were consequently able to punch through cool, dense porewater bodies resident in the shallow sediments to reach the seafloor. Elsewhere (e.g. Lisheen, Galmoy, Navan), dense shallow brines may have impeded venting with possible late stage exhalation at Navan linked to unroofing of the deposit due to major tectonic instability and submarine gravity sliding during development of the Boulder Conglomerate (Ashton et al., 1986).

In terms of their T_h-salinity properties, the fluids associated with the MVT deposits are distinct and do not clearly fit the broader regional pattern (Fig. 9). It is noteworthy that the principal area in which these deposits are observed is spatially associated with a low in the regional vitrinite/CAI maturity data. This relationship suggests that this region has not undergone the same subsidence and higher temperature fluid flow history as much of the rest of the Midlands and is consequently suggested to be not prospective for true Irish-type deposits (*sensu* Wilkinson, 2003).

Brine origins

904   Seawater evaporation to varying degrees played a key role in the generation of orefluids for the

905   Irish Zn-Pb deposits. The principal orefluids were produced from partially evaporated seawater; there

906   is no evidence for the involvement of brines produced by halite dissolution as would probably be

907   required in the lateral flow models driven by Variscan topographic relief (e.g., Hitzman and Beaty,

908   1996). An interesting question is why only these partially evaporated fluids appear to have circulated

909   to depth. It could be due to the paleogeography, with recharge areas only tapping marine waters

910   from partially restricted sub-basins and not from areas of high evaporation (Fig. 10). A complex

911   paleogeographic control on brine evolution has been recognized in studies of recent intracratonic

912   marine basins such as the Dead Sea (Klein-BenDavid et al., 2004). Alternatively, more strongly

913   evaporated brines may also have circulated into the basement but were too dense to undergo return

914   buoyant flow to the near-surface.

915   More strongly evaporated brines were widespread, but these are only recognized in the Lower

916   Carboniferous succession, with the exception of the small component inferred to be present in the

917   LP_{1b} fluids. Three brine types have been identified, all enriched in Ca: (B_1) relatively high Na# (~0.8)

918   brines associated with pink dolomite; (B_2) more saline brines with elevated Ca (Na# ~0.5) associated

919   with pervasive dolomitization; and more calcic brines (Na# ~0.6-0.2), associated with dolomitization

920   of shelf limestones. Evaporation of modern seawater only produces very low Ca brines due to the

921   precipitation of gypsum and an excess of SO_4^{2-} over Ca^{2+}. The observed variable enrichments in Ca are

922   therefore most likely due to Ca gain, possibly via gypsum dissolution and, probably more likely, Ca-

923   Mg exchange dolomitization. Mole-for-mole replacement of Ca by Mg results in net volume

924   reduction (ΔV = -9.74 cm^3 mol^{-1}; -13%), consistent with the observation of increasing porosity and

925   development of coarse, euhedral saddle dolomite during progressive dolomitization. Similar fluid-

926   rock interactions have been suggested for the origin of Ca chloride brines in the Dead Sea Rift (e.g.

927   Stein et al., 2000).

928

929   *Role of fluid mixing*

930   In Ireland, ore formed at the interface between deeply-circulating and shallow, diagenetic flow

931   systems (e.g. Wilkinson et al., 2005a) within carbonate host rocks, with mixing being an important

932   process that allowed low-sulfur, metal-rich fluids to saturate with sulfides and at the same time

933   generate porosity for sulfide deposition. However, fluid inclusion data suggest that mixing also

934   occurred in other parts of the flow system that, in combination with the variety of fluid types

935   potentially involved (seawater, variably evaporated seawater, exchanged variably evaporated

936   seawater, bittern brines), resulted in significant complexity in fluid chemistry. In the Lower Paleozoic

937   basement there is evidence for mixing of Br-enriched brine with partially evaporated, extensively

938   exchanged seawater as the latter fluids ascended toward the paleoseafloor. The rare occurrence of

939 barite in Lower Paleozoic-hosted veins with a Carboniferous seawater sulfate signature (Everett,

940 1999), pyrite with low (ore-like) $\delta^{34}S$ values, and variations in Na# in fluid inclusions are consistent

941 with minor LP_1-brine mixing within at least the upper parts of the basement sequence.

942 Mixing of LP_2 fluids with brines in the ore-forming environment appears to have been an

943 important depositional mechanism and the halogen data suggest that Br-enriched bittern brines

944 were involved. These brines must have become enriched in reduced sulfur by bacteriogenic

945 reduction (e.g. Boyce et al., 1983; Caulfield et al., 1986) prior to mixing. It is suggested that the

946 development of submarine hot springs and/or seeps above major hydrothermal plumes resulted in

947 the local development of chemosynthetic faunal communities including abundant sulfate-reducing

948 bacteria. These bacterial blooms could have concentrated H_2S in brines trapped in seafloor

949 depressions and in underlying lithologies proximal to hydrothermal upflow zones. In the Waulsortian-

950 hosted deposits, these sulfidic brines could have been resident within permeable Waulsortian that

951 had been previously dolomitized (e.g. Lisheen, Galmoy; Wilkinson et al., 2005b) or in sedimentary

952 slump breccias in undolomitized Waulsortian (e.g. Silvermines; Lee and Wilkinson, 2002), perched on

953 the relatively impermeable underlying argillaceous limestones. Mixing along the interface between

954 such brine lenses and upwelling LP_2 fluids is consistent with the observation that the base of massive

955 sulfide is often planar, horizontal and commonly transgresses stratigraphy. Furthermore, the contact

956 between hydrothermal black dolomite cemented breccias (formed at the mixing interface) and

957 overlying white matrix breccias (cement precipitated from largely unmodified LP_2 fluids) is

958 subhorizontal and sharp to gradational over a few meters (Hitzman et al., 2002; Lee and Wilkinson,

959 2002; Fusciardi et al., 2003).

960 Fluid inclusion data show that, generally, hydrothermal dolomite was precipitated at the highest

961 temperatures, probably during the first increments of fluid mixing. The lack of Mg in the LP fluids

962 indicates that mixing with unexchanged, Mg-rich brines is likely to be essential for extensive dolomite

963 development in areas where pre-existing diagenetic dolomite was not abundant (e.g., Silvermines:

964 Lee and Wilkinson, 2002). In the south and east Midlands, where early pervasive dolomitization of

965 the Waulsortian had occurred (Hitzman, 1995), local recrystallization could have supplied some of

966 the required Mg.

967 Across the orefield, sphalerite-hosted inclusions tend to form relatively tight clusters of data from

968 individual samples and be polymodal in terms of salinity. The reason for this is uncertain although it

969 is suggested that the more crystalline sphalerite samples amenable to inclusion analysis may

970 represent pockets of mixed fluid that precipitated sphalerite during cooling in the waning stages of

971 individual pulses of hydrothermal fluid ingress. Finer-grained sphalerite types probably precipitated

972 over a greater part of any mixing interval but the fluid inclusion record of this is only (partly)

973 preserved in the coexisting gangue. The salinity modes observed may reflect different degrees of

974   mixing but the occurrence of comparable modes in different deposits as well as in basement-hosted

975   veins (Table 1; Wilkinson et al., 2009) suggests that infiltration of LP fluids of varying salinity and

976   composition occurred at different times as well as in space. The majority of sphalerite in the

977   Waulsortian-hosted systems appears to be associated with the more saline mode(s), suggesting that

978   this (presumably more highly evaporated) interacted seawater was particularly important for ore

979   formation (Wilkinson et al., 2009).

980   Calcite appears to have been more commonly precipitated during extensive mixing and at lower

981   temperatures, although some high temperature, unmixed, fluids are responsible for the formation of

982   calcite feeder veins in some of the deposit footwalls (e.g., Silvermines: Lee and Wilkinson, 2002).

983   At Lisheen, Galmoy, Silvermines (Cooleen Zone), Castlegarde and Keel, a trend toward more

984   dilute, lower T_h inclusions has been recognized, consistent with mixing between LP fluids and low

985   temperature seawater. It is perhaps not suprising that this is observed given the inferred near-

986   seafloor environment of ore-formation. Evidence from Silvermines suggests that such mixing tends

987   to be restricted to the margins of the system, outside the region of brine influence. It is suggested

988   that upwelling orefluids may have been deflected around a dense brine lens, mixing along the

989   interface with brine and then being diluted by normal seawater along the margins (Fig. 10). Although

990   seawater mixing does appear to be capable of driving fluids to sulfide saturation (presumably via

991   cooling and decreased ligand concentration), it is not thought to be favourable for extensive sulfide

992   deposition due to the limited sulfur supply in the LP fluids. The predominance of deep, hydrothermal

993   sulfur in these zones is confirmed by the high (>0) δ^{34}S values observed in the subeconomic Cooleen

994   Zone at Silvermines (Lee, 2002).

995   The subeconomic prospects generally appear to show a restricted salinity range, being dominated

996   by LP fluids that vary widely in temperature between localities. At present, it is not known if the

997   prospects formed from LP fluids with less (LP$_1$) or more (LP$_2$) exchanged character. Dilution trends

998   are observed in some of the prospects (e.g., Castlegarde, Cooleen, Keel), but the brine mixing trends

999   that appear to be consistently observed in the ore deposits are weak or absent. Thus, LP-brine mixing

1000   is one of the key factors that appears to be missing from the subeconomic systems. The low

1001   temperature, possibly slightly younger, MVT deposits show some evidence of mixing but lack the

1002   elevated temperatures that may be required for significant metal solubilization and show little

1003   evidence of the bacteriogenic sulfide trap, being typified by positive δ^{34}S values (Dixon, 1990).

1004   Cooling, neutralization due to extensive retrograde carbonate dissolution, and inorganic sulfate

1005   reduction are suggested as the controls of sulfide deposition from these late, cool, LP-type fluids that

1006   are interpreted to reflect the waning phase of the convective flow system.

1007   The formation of economic mineralization in Ireland appears to reflect the coincidence of high

1008   temperature reaction zones in the basement, brine-producing footwalls, and hangingwall structural-

1009   stratigraphic traps, with bacterial blooms linked to upwelling plumes of hydrothermal fluids. The ore

1010   deposits can therefore be viewed as products of self-organizing systems – with a first-order structural

1011   control – that locally converged on ore-forming conditions. Understanding the basement structural

1012   architecture will therefore be critical for predicting new deposits.

1013

1014   *Wider implications*

1015   The Irish hydrothermal system shares much of the variety and complexity observed in other

1016   intracratonic basin-hosted Zn-Pb(-Ba) ore districts. This includes the coexistence of contrasting styles

1017   of mineralization that are typically observed in the more distal and platform-marginal parts of the

1018   basinal environment (Sangster, 1990). In Ireland, true Irish-type (carbonate-hosted, stratiform-

1019   stratabound, massive sulfide replacement ore deposits) and MVT deposits are linked by the same

1020   type of fluids, but the MVT deposits display distinct morphologies and chemical characteristics that

1021   are related to their likely younger age, lower temperature of formation, and lack of a bacteriogenic

1022   sulfide trap. Specific characteristics include: non-stratiform breccia geometry, crustiform clast

1023   coatings, high Zn/Pb, dendritic galena, presence of melnikovite, abundance of marcasite-calcite,

1024   finely banded colloform sphalerite, and pale crystalline sphalerite. Higher temperature (Irish-type)

1025   indicators include: stratiform sulfide and (where present) breccia body geometry, massive sulfide

1026   texture, high Ni and Cd, low Zn/Pb, dark crystalline sphalerite, chalcopyrite, tennantite and other

1027   sulfosalts.

1028   The Irish-type ore deposits can be viewed as intermediate between classic shale-hosted, deeper

1029   water Sedex deposits and platform carbonate-hosted MVT deposits in that they formed in a ramp

1030   environment beneath water depths of up to several hundred meters; they formed at around the

1031   time of host rock deposition to up to ~10 My later; and they are hosted by carbonates within a

1032   carbonate-shale sequence. The deposits were probably produced by convective flow systems that

1033   developed many of the geological features more commonly associated with Sedex than with MVT

1034   deposits, including higher fluid temperatures and lower salinities, footwall (classic epigenetic) feeder

1035   vein and breccia zones, and strong zoning on the deposit scale in terms of metals and alteration

1036   patterns (e.g., Ashton et al., 1992; Fusciardi et al., 2003; Lowther et al., 2003). The recognition of

1037   significant heterogeneity in fluid chemistry in Ireland (and in the metal tenor of resulting deposits)

1038   may reflect an intrinsic character of convective flow systems that might be anticipated in other Sedex

1039   provinces.

1040   The derivation of a range of components from the underlying low-grade metamorphic basement

1041   can be convincingly demonstrated (Pb, Sr) or inferred (Li, Ca, Ba, Mn, Fe, Co, Ni, Cu, Zn, As). Fluids

1042   flowing within extensive fracture permeability in this metal-fertile, arc-derived greywacke-shale

1043   (±volcanic) succession are clearly capable of efficiently extracting metals. This implies that basement

1044 involvement could be important in other sediment-hosted systems, and the common assumption

1045 that fluids and metals are solely derived from basinal clastic successions (e.g., Goodfellow et al.,

1046 1993; Leach et al., 2005) should be tested critically. The potential for surficial recharge of fluids, as

1047 documented in Ireland, means that the system is not intrinsically fluid volume-limited enabling

1048 potentially greater metal mobilization. Such deep crustal circulation is probably a requirement in

1049 basin environments where subsidence has been limited and basin successions are consequently thin;

1050 however, it may not be required in long-lived intracratonic basins (typified by many Proterozoic

1051 systems), where basin sequences may be in excess of 10 km.

1052   A complex evolution in pore fluid chemistry in the carbonate host rocks can be documented from

1053 early, seawater-related diagenetic fluids (based mainly on textures and marine carbon and oxygen

1054 isotope signatures) that were replaced by progressively hotter hydrothermal fluids (from textures

1055 and fluid inclusion, carbon, oxygen and strontium isotope data). Later brines then dolomitized

1056 younger sediments and overprinted the ore deposits. All these fluids were derived ultimately from

1057 seawater, and the ambient paleoclimate and paleotopography played a key role in controlling fluid

1058 heterogeneity and possibly fluid fertility, as well as recharge. The evolution of brine chemistry and

1059 the flow pathways utilized are likely to be a function of the detailed paleogeography/

1060 geomorphology, distribution and diagenesis of sedimentary facies, and basin floor/margin

1061 permeability as is highlighted in studies of modern intracratonic basins (e.g. Stanislavsky and

1062 Gvirtzman, 1999; Stein et al., 2000; Klein-BenDavid et al., 2004). Consequently, significant complexity

1063 should be expected in fluid origins in intracratonic basin-hosted ore districts elsewhere, but these

1064 can be resolved with careful application of modern microchemical analyses of fluid inclusions.

1065

1066 *Concluding remarks*

1067   The Irish orefield presents arguably the best database available on the thermal and chemical

1068 characteristics of hydrothermal fluids involved in sediment-hosted ore genesis and is an excellent

1069 example of a fossil, crustal scale hydrothermal system. As such, it provides a valuable laboratory that

1070 could be used for further understanding the dynamics of flow, the chemical exchange and the origin,

1071 transport and deposition of metals during seawater-crust interaction. Outcrop access to various parts

1072 of the stratigraphic record in Ireland, coupled with mine exposures and extensive drillcore has

1073 allowed a three dimensional understanding of the hydrothermal system to be developed. Fluid

1074 inclusion measurements, together with careful paragenetic studies that require the use of detailed

1075 textural analytical tools such as cathodoluminescence, have allowed the system to be examined as a

1076 function of relative time. Future geochronology is desirable, although the interpretation of

1077 increasingly precise geochonological ages will remain problematic in the absence of finely resolved

1078 stratigraphic dating in the Lower Carboniferous. Regional-scale sampling has identified large-scale

1079   heterogeneity in fluid properties and the data indicate complex fluid-fluid and fluid-rock interaction

1080   processes at the local scale. Although a start has been made, further work comparing and

1081   interpreting thermal, chemical and isotopic tracers in the ore systems with those in weakly

1082   mineralized prospects is needed to better understand the processes controlling the localization of

1083   economic mineralization.

1084

1102 **References**

1103

1104 Agrinier, P., Hékinian, R., Bideau, D., and Javoy, M., 1995, O and H stable isotope compositions of

1105 oceanic crust and upper mantle rocks exposed in the Hess Deep near the Galapagos Triple Junction:

1106 Earth and Planetary Science Letters, v. 136, p. 183-196.

1107

1108 Allan, J.R., Beaty, D.W., Sturtevant, R.G., Hitzman, M.W., and Shearley, E., 1992, The origin of

1109 regional dolomite in the Waulsortian of southeastern Ireland: implications for ore deposition [abs]:

1110 Geological Society of America, Abstracts with Programs, v. 24, p. A354.

1111

1112 Anderson, I.K., Ashton, J.H., Earls, G., Hitzman, M.W., and Tear, S., eds., 1995, Irish Carbonate-hosted

1113 Zn-Pb Deposits. Society of Economic Geologists Guidebook Series, Volume 21.

1114

1115 Anderson, I.K., Ashton, J.H., Boyce, A.J., Fallick, A.E., and Russell, M.J., 1998, Ore depositional

1116 processes in the Navan Zn + Pb deposit, Ireland: ECONOMIC GEOLOGY, v. 93, p. 535-563.

1117

1118 Andrew, C.J., 1993, Mineralization in the Irish Midlands, in Pattrick, R.A.D. and Polya, D.A., eds.,

1119 Mineralization in the British Isles: London, Chapman and Hall, p. 208-269.

1120

1121 Andrew, C.J., Crowe, R.W.A., Finlay, S., Pennell, W.M., and Pyne, J., eds., 1986, Geology and genesis

1122 of mineral deposits in Ireland: Dublin, Irish Association for Economic Geology, 711 pp.

1123

1124 Ashton, J.H., Downing, D.T., and Finlay, S., 1986, The geology of the Navan Zn-Pb orebody, in Andrew,

1125 C.J., Crowe, R.W.A., Finlay, S., Pennell, W.M. and Pyne, J., eds., Geology and genesis of mineral

1126 deposits in Ireland: Dublin, Irish Association for Economic Geology, p. 243-280.

1127

1128 Ashton, J.H., Black, A., Geraghty, J., Holdstock, M., and Hyland, E., 1992, The geological setting and

1129 metal distribution patterns of Zn-Pb-Fe mineralization in the Navan Boulder Conglomerate, in

1130 Bowden, A.A., Earls, G., O'Connor, P.G., and Pyne, J.F., eds., The Irish Minerals Industry 1980-1990:

1131 Dublin, Irish Association for Economic Geology, p. 171-197.

1132

1133 Banks, D.A., 1985, A fossil hydrothermal worm assemblage from the Tynagh lead-zinc deposit in

1134 Ireland: Nature, v. 313, p. 128-131.

1135

1136   Banks, D.A., and Russell, M.J., 1992, Fluid mixing during ore deposition at the Tynagh base metal

1137   deposit, Ireland: European Journal of Mineralogy, v. 4, p. 921-931.

1138

1139   Banks, D.A., Boyce, A.J., and Samson, I.M., 2002, Constraints on the Origins of fluids forming Irish Zn-

1140   Pb-Ba deposits: Evidence from the composition of fluid Inclusions: ECONOMIC GEOLOGY, v. 97, p.

1141   471-480.

1142

1143   Blakeman, R., Ashton, J.H., Boyce, A.J., Fallick, A.E., and Russell, M.J., 2002, Timing of interplay

1144   between hydrothermal and surface fluids in the Navan Zn+Pb orebody, Ireland: Evidence from metal

1145   distribution trends, mineral textures and δ^{34}S analyses: ECONOMIC GEOLOGY, v. 97, p. 73-91.

1146

1147   Boast, A.M., Coleman, M.L., and Halls, C., 1981, Textural and stable isotopic evidence for the genesis

1148   of the Tynagh base metal deposit, Ireland: ECONOMIC GEOLOGY, v. 76, p. 27-55.

1149

1150   Bodnar, R.J., 2003a, Re-equilibration of fluid inclusions, in Samson, I., Anderson, A., and Marshall, D.,

1151   eds., Fluid Inclusions: Analysis and Interpretation: Mineralogical Association of Canada Short Course

1152   32, Chapter 4.

1153

1154   Bodnar, R.J., 2003b, Interpretation of data from aqueous-electrolyte fluid inclusions, in Samson, I.,

1155   Anderson, A., and Marshall, D., eds., Fluid Inclusions: Analysis and Interpretation: Mineralogical

1156   Association of Canada Short Course 32, Chapter 8.

1157

1158   Bodnar, R.J., and Bethke, P.M., 1984, Systematics of stretching of fluid inclusions I: Fluorite and

1159   sphalerite at 1 atmosphere confining pressure: ECONOMIC GEOLOGY, v. 79, p. 141-161.

1160

1161   Bodnar, R.J., Binns, P.R., and Hall, D.L., 1989, Synthetic fluid inclusions – VI. Quantitative evaluation

1162   of the decrepitation behaviour of fluid inclusions in quartz at one atmosphere confining pressure:

1163   Journal of Metamorphic Geology, v. 7, p. 229-242.

1164

1165   Bowden, A.A., Earls, G., O'Connor, P.G., and Pyne, J.F., eds., 1992, The Irish Minerals Industry 1980-

1166   1990: Dublin, Irish Association for Economic Geology, 434 p.

1167

1168   Boyce, A.J., Anderton, R., and Russell, M.J., 1983, Rapid subsidence and early Carboniferous

1169   mineralisation in Ireland: Transactions of the Institution of Mining and Metallurgy, v. 92, p. B55-66.

1170

1171 Boyce, A.J., Little, C.T.S., and Russell, M.J., 2003, A new fossil vent biota in the Ballynoe barite

1172 deposit, Silvermines, Ireland: Evidence for intracratonic sea-floor hydrothermal activity about 352

1173 Ma: ECONOMIC GEOLOGY, v. 98, p. 649-656.

1174

1175 Burruss, R.C., 1987, Diagenetic palaeotemperatures from aqueous fluid inclusions: re-equilibration of

1176 inclusions in carbonate cements by burial heating: Mineralogical Magazine, v. 51, p. 477-481.

1177

1178 Caulfield, J.B.D., LeHuray, A.P., and Rye, D.M., 1986, A review of lead and sulphur isotope

1179 investigations of Irish sediment-hosted base metal deposits, with new data from Keel, Ballinalack,

1180 Moyvoughly and Tatestown deposits, in Andrew, C.J., Crowe, R.W.A., Finlay, S., Pennell, W.M., and

1181 Pyne, J., eds., Geology and genesis of mineral deposits in Ireland: Dublin, Irish Association for

1182 Economic Geology, p. 591-616.

1183

1184 Clayton, G., Haughey, N., Sevastopulo, G.D., and Burnett, R., 1989, Thermal maturation levels in the

1185 Devonian and Carboniferous rocks in Ireland. Dublin, Geological Survey of Ireland, 36 p.

1186

1187 Corbett, G., 2004, Epithermal and porphyry gold – Geological models, in Proceedings of the PACRIM

1188 2004 Congress, Adelaide: Melbourne, Australian Institute of Mining and metallurgy, p. 15-23.

1189

1190 Crowther, H.L., 2007, A rare earth element and transition metal isotope study of the Irish Zn-Pb

1191 orefield: Unpub. Ph.D. thesis, University of London, 198 p.

1192

1193 Dix, G.R., and Edwards, C., 1996, Carbonate-hosted, shallow-submarine and burial hydrothermal

1194 mineralization in the Upper Mississippian Big Cove Formation, Port au Port Peninsula,

1195 Western Newfoundland: ECONOMIC GEOLOGY, v. 91, p. 180-203.

1196

1197 Dixon, P.R., 1990, The role of basement-circulated fluids in the origin of sediment-hosted Zn-Pb-Ba

1198 mineralization in Ireland: Unpub. Ph.D. thesis, Yale University, 249 p.

1199

1200 Doyle, E., Bowden, A.A., Jones, G.V., and Stanley, G.A., 1992, The geology of the Galmoy deposits, in

1201 Bowden, A.A., Earls, G., O'Connor, P.G., and Pyne, J.F., eds., The Irish Minerals Industry 1980-1990:

1202 Dublin, Irish Association for Economic Geology, p. 211-225.

1203

1204   Emo, G.T., 1986, Some considerations regarding the styles of mineralization at Harberton Bridge, Co.
1205   Kildare, in Andrew, C. J., Crowe, R. W. A., Finlay, S., Pennell, W. M. and Pyne, J., eds., Geology and
1206   genesis of mineral deposits in Ireland: Dublin, Irish Association for Economic Geology, p. 461-470.
1207

1208   Everett, C.E., 1999, Tracing ancient fluid flow pathways: A study of the Lower Carboniferous base
1209   metal orefield in Ireland: Unpub. Ph.D. thesis, Yale Univ., 354 p.
1210

1211   Everett C.E., Wilkinson, J.J., and Rye, D.M., 1999a, Fracture-controlled fluid flow in the Lower
1212   Palaeozoic basement rocks of Ireland: Implications for the genesis of Irish-type Zn-Pb deposits, in
1213   McCaffrey, K.J.W., Lonergan, L. and Wilkinson, J.J., eds., Fractures, Fluid Flow and Mineralization:
1214   Geological Society of London, Special Publications, v. 155, p. 247-276.
1215

1216   Everett, C.E., Wilkinson, J.J., Boyce, A.J., Ellam R., Gleeson, S.A., Rye, D.M., and Fallick, A.E., 1999b,
1217   The genesis of Irish-type base metal deposits: Characteristics and origins of the principal ore fluid, in
1218   Stanley, C.J. et al., eds., Mineral Deposits; Processes to Processing: Rotterdam, A.A. Balkema, p. 845-
1219   848.
1220

1221   Everett, C.E., Rye, D.M., and Ellam, R.M., 2003, Source or sink? An assessment of the role of the Old
1222   Red Sandstone in the genesis of the Irish Zn-Pb deposits: ECONOMIC GEOLOGY, v. 98, p. 31-50.
1223

1224   Eyre, S.L., 1998, Geochemistry of dolomitization and Zn-Pb mineralization in the Rathdowney Trend,
1225   Ireland: Unpub. Ph.D. thesis, Univ. London, 414 p.
1226

1227   Eyre, S.L., Wilkinson, J.J., Stanley, C.J., Boyce, A.J., 1996, Geochemistry of dolomitisation and zinc-
1228   lead mineralisation in the Rathdowney Trend, Ireland [abs]: Geological Society of America, Abstracts
1229   with Programs, v. 28, p. A210-211.
1230

1231   Fournier, R.H., and Truesdell, A.H., 1973, An empirical Na-K-Ca geothermometer for natural waters.
1232   Geochimica et Cosmochimica Acta, v. 37, p. 1255-1275.
1233

1234   Fusciardi, L.P., Guven, J.F., Stewart, D.R.A., Carboni, V., and Walshe, J.J., 2003, The geology and
1235   genesis of the Lisheen Zn-Pb deposit, Co. Tipperary, Ireland, in Kelly, J.G., Andrew, C.J., Ashton, J.H.,
1236   Boland, M.B., Earls, G., Fusciardi, L., and Stanley, G., eds., Europe's Major Base Metal Deposits:
1237   Dublin, Irish Association for Economic Geology, p. 455-481.
1238

1239   Giggenbach, W.F., 1988, Geothermal solute equilibria. Derivation of Na-K-Mg-Ca geoindicators.

1240   Geochimica et Cosmochimica Acta, v. 52, p. 2749-2765.

1241

1242   Gleeson, S.A., Banks, D.A., Everett, C.E., Wilkinson, J.J., Samson, I.M., and Boyce, A.J., 1999, Origin of

1243   mineralising fluids in Irish-type deposits: constraints from halogen analyses, in Stanley, C.J. et al.,

1244   eds., Mineral Deposits; Processes to Processing: Rotterdam, A.A. Balkema, p. 857-860.

1245

1246   Gleeson, S.A., Wilkinson, J.J., Stuart, F.M., and Banks, D.A., 2001, The origin and chemical evolution

1247   of base metal mineralising formation waters and hydrothermal fluids, South Cornwall, U.K.:

1248   Geochimica et Cosmochimica Acta, v. 65, p. 2067-2079.

1249

1250   Goodfellow, W.D., Lydon, J.W., and Turner, R.W., 1993, Geology and genesis of stratiform sediment-

1251   hosted (SEDEX) Zn-Pb-Ag sulphide deposits: Geological Association of Canada, Special Paper 40, p.

1252   201-251.

1253

1254   Goodhue, R., and Clayton, G., 1999, Organic maturation levels, thermal history and hydrocarbon

1255   source rock potential of the Namurian rocks of the Clare Basin, Ireland: Marine and Petroleum

1256   Geology, v. 16, p. 667-675.

1257

1258   Gregg, J.M., Shelton, K.L., Johnson, A.W., Somerville, I.D., and Wright, W.R., 2001, Dolomitization of

1259   the Waulsortian Limestone (Lower Carboniferous) in the Irish Midlands: Sedimentology, v. 48, p. 745-

1260   766.

1261

1262   Greig, J.A., Baadsgard, H., Cumming, G.L., Folinsbee, R.E., Krouse, H.R., Ohmoto, H., Sasaki, A. and

1263   Smejkal, V., 1971, Lead and sulfur isotopes of the Irish base metal mines in Carboniferous carbonate

1264   host rocks: Proceedings of the joint IMA-IAGOD meeting, Tokyo, 1970. Society of Mining Geologists

1265   of Japan, Special Issue No. 2, p. 84-92.

1266

1267   Grennan, E.F., 1986, Geology and genesis of the Courtbrown Pb-Zn-Ag deposit, in Andrew, C.J.,

1268   Crowe, R.W.A., Finlay, S., Pennell, W.M. and Pyne, J., eds., Geology and genesis of mineral deposits in

1269   Ireland: Dublin, Irish Association for Economic Geology, p. 449-455.

1270

1271   Hitzman, M.W., 1986, Geology of the Abbeytown Mine, Co. Sligo, Ireland, in Andrew C.J., Crowe,

1272   R.W.A., Finlay, S., Pennell, W.M., and Pyne, J., eds., Geology and genesis of mineral deposits in

1273   Ireland: Dublin, Irish Association for Economic Geology, p. 341-353.

1274

1275   Hitzman, M.W., 1995, Geological setting of the Irish Zn-Pb-(Ba-Ag) orefield, in Anderson, I.K., Ashton,

1276   J.H., Earls, G., Hitzman, M.W., and Tear, S., eds., Irish Carbonate-hosted Zn-Pb Deposits: Society of

1277   Economic Geologists Guidebook Series, v. 21, p. 3-23.

1278

1279   Hitzman, M.W. and Beaty, D.W., 1996, The Irish Zn-Pb-(Ba) orefield, in Sangster, D.F., ed., Carbonate-

1280   hosted lead-zinc deposits: Society of Economic Geologists, Special Publication, v. 4, p. 112-143.

1281

1282   Hitzman, M.W., and Large, D.E., 1986, A review and classification of the Irish carbonate-hosted base

1283   metal deposits, in Andrew, C.J., Crowe, R.W.A., Finlay, S., Pennell, W.M., and Pyne, J., eds., Geology

1284   and genesis of mineral deposits in Ireland: Dublin, Irish Association for Economic Geology, p. 217-

1285   238.

1286

1287   Hitzman, M.W., O'Connor, P.G., Shearley, E., Schaffalitzky, C., Beatty, D.W., Allan, J.R., and

1288   Thompson, T., 1992, Discovery and geology of the Lisheen Zn-Pb-Ag prospect, Rathdowney Trend,

1289   Ireland, in Bowden, A.A., Earls, G., O'Connor, P.G., and Pyne, J.F., eds., The Irish Minerals Industry

1290   1980-1990: Dublin, Irish Association for Economic Geology, p. 227-246.

1291

1292   Hitzman, M.W., Earls, G., Shearley, E.,Kelly, J., Cruise, M., and Sevastopulo, G., 1995, Ironstones (iron

1293   oxide-silica) in the Irish Zn-Pb deposits and regional iron oxide-(silica) alteration of the Waulsortian

1294   limestone in southern Ireland, in Anderson, I.K., Ashton, J.H., Earls, G., Hitzman, M.W., and Tear, S.,

1295   eds., Irish Carbonate-hosted Zn-Pb Deposits: Society of Economic Geologists Guidebook Series, v. 21,

1296   p. 261-273.

1297

1298   Hitzman, M.W., Allan, J.R., and Beaty, D.W., 1998, Regional dolomitization of the Waulsortian

1299   limestone in southeastern Ireland: evidence of large-scale fluid flow driven by the Hercynian

1300   orogeny: Geology, v. 26, p. 547-550.

1301

1302   Hitzman, M.W., Redmond, P.B., and Beaty, D.W., 2002, The carbonate-hosted Lisheen Zn-Pb-Ag

1303   deposit, County Tipperary, Ireland: ECONOMIC GEOLOGY, v. 97, p. 1627-1655.

1304

1305   Holdstock, M.P., 1982, Breccia hosted zinc-lead mineralization in Tournasian and Lower Visean

1306   carbonates at Harberton Bridge, Co. Kildare, in Brown, A.G., ed., Mineral Exploration in Ireland,

1307   Progress and Developments 1971-1981: Dublin, Irish Association for Economic Geology, p. 83-91.

1308

1309 Holdstock, M.P., 1983, The Lower Carboniferous geology and base metal mineralization of northeast
1310 County Kildare, Ireland. Unpub. Ph.D. thesis, National University of Ireland.

1311

1312 Johnson, A.W., Shelton, K.L., Gregg, J.M., Somerville, I.D., and Wright, W.R., 2001, Fluid inclusion
1313 evidence for the presence of multiple fluids in Zn-Pb hosting carbonate rocks in the Irish Midlands:
1314 Initial findings, in Hagni, R.D., ed., Studies on ore deposits, mineral economics and applied
1315 mineralogy: University of Missouri-Rolla, p. 18-30.

1316

1317 Johnson, A.W., Shelton, K.L., Gregg, J.M., Somerville, I.D., Wright, W.R., and Nagy, Z.R., 2009,
1318 Regional studies of dolomites and their included fluids: recognizing multiple chemically distinct fluids
1319 during the complex diagenetic history of Lower Carboniferous (Mississippian) rocks of the Irish Zn-Pb
1320 ore field: Mineralogy and Petrology, DOI 10.1007/s00710-008-0038-x.

1321

1322 Jones, G.Ll., 1992, Irish Carboniferous conodonts record maturation levels and the influence of
1323 tectonism, igneous activity and mineralization: Terra Nova, v. 4, p. 228-234.

1324

1325 Kelly, J.G., Andrew, C.J., Ashton, J.H., Boland, M.B., Earls, G., Fusciardi, L., and Stanley, G., eds., 2003,
1326 Europe's Major Base Metal Deposits: Dublin, Irish Association for Economic Geology, 552 p.

1327

1328 Kennan, P.S., Phillips, W.E.A. and Strogen, P., 1979, Pre-Caledonian basement to the paratectonic
1329 Caledonides in Ireland: Geological Society of London, Special Publications, v. 8, p. 157-161.

1330

1331 Klein-BenDavid, O., Sass, E., and Katz, A., 2004, The evolution of marine evaporitic brines in inland
1332 basins: The Jordan–Dead Sea Rift valley: Geochimica et Cosmochimica Acta, v. 68, p. 1763-1775.

1333

1334 Knauth, L.P., and Beeunas, M.A., 1985, Isotope geochemistry of fluid inclusions in Permian halite with
1335 implications for the isotopic history of ocean water and the origin of saline formation waters:
1336 Geochimica et Cosmochimica Acta, v. 50, p. 419-433.

1337

1338 Leach, D.L., Sangster, D.L., Kelley, K.D., Large, R.R., Garven, G., Allen, C.R., Gutzmer, J., and Walter, S.,
1339 2005, Sediment-hosted lead-zinc deposits: A global perspective: Society of Economic Geologists, One
1340 Hundredth Anniversary Volume 1905-2005, p. 561-607.

1341

1342 Lee, M.J., 2002, Origin and Zn-Pb mineralization of dolomite breccias in the Irish Midlands: Unpub.
1343 Ph.D. thesis, Univ. London, 256 p.

1344

1345   Lee, M.J., and Wilkinson, J.J., 2002, Cementation, hydrothermal alteration, and Zn-Pb mineralization

1346   of carbonate breccias in the Irish Midlands: Textural evidence from the Cooleen Zone, near

1347   Silvermines, County Tipperary: ECONOMIC GEOLOGY, v. 97, p. 653-662.

1348

1349   Lees, A., and Miller, J., 1995, Waulsortian banks, in Monty, C.L.V., Bosence, D.W.J., Bridges, P.H., and

1350   Pratt, B.R., eds., Carbonate Mud-Mounds: Oxford, Blackwell Science, International Association of

1351   Sedimentologists Special Publication 23, p. 191-271.

1352

1353   Lepp, H., 1957, The synthesis and probable geologic significance of melnikovite: ECONOMIC

1354   GEOLOGY, v. 52, p. 528-535.

1355   Lowenstein, T.K., Hardie, L.A., Timofeeff, M.N., and Demicco, R.V., 2003, Secular variation in

1356   seawater chemistry and the origin of calcium chloride basinal brines: Geology, v. 31, p. 857-860.

1357

1358   Lowther, J.M., Balding, A.B., McEvoy, F.M., Dunphy, S., MacEoin, P., Bowden, A.A., and McDermott,

1359   P., 2003, The Galmoy Zn-Pb orebodies: structure and metal distribution – clues to the genesis of the

1360   deposits, in Kelly, J.G., Andrew, C.J., Ashton, J.H., Boland, M.B., Earls, G., Fusciardi, L., and Stanley, G.,

1361   eds., Europe's Major Base Metal Deposits: Dublin, Irish Association for Economic Geology, p. 437-

1362   454.

1363

1364   Lydon, J. W., 1986, A model for the generation of metalliferous hydrothermal solutions in a

1365   sedimentary basin, and its application to the Irish Carboniferous base metal deposits, in Andrew, C.

1366   J., Crowe, R. W. A., Finlay, S., Pennell, W. M. and Pyne, J., eds., Geology and genesis of mineral

1367   deposits in Ireland: Dublin, Irish Association for Economic Geology, p. 555-577.

1368

1369   McCaffrey, M.A., Lazar, B., and Holland, H.D., 1987, The evaporation path of seawater and the

1370   coprecipitation of Br^- and K^+ with halite: Journal of Sedimentary Petrology, v. 57, p. 928-937.

1371

1372   Mulhall, C.M., 2003, An investigation of the fluids involved in the formation of some Irish Lower

1373   Carboniferous dolomites: Unpub. Ph.D. thesis, Trinity College Dublin, 325 p.

1374

1375   Naden, J., 1996. CalcicBrine 1.5: a Microsoft Excel 5.0 add-in for calculating salinities from

1376   microthermometric data in the system $NaCl-CaCl_2-H_2O$ [abs]: PACROFI VI, Abstracts Volume,

1377   University of Wisconsin, Madison, USA, p. 97-98.

1378

1379 Nagy, Z.R., Gregg, J.M., Becker, S.P., Somerville, I.D., Shelton, K.L., and Johnson, A.W., 2004, Early
1380 dolomitisation and fluid migration through the Lower Carboniferous carbonate platform in the
1381 southeast Irish Midlands: Implications for reservoir attributes, in Braithwaite C.J.R., Rizzi G., and
1382 Darke G., eds., The Geometry and Petrogenesis of Dolomite Hydrocarbon Reservoirs: Geological
1383 Society of London, Special Publications, v. 235, p. 367-392.
1384
1385 Nunn, J.A., 1994, Free thermal convection beneath intracratonic basins: thermal and subsidence
1386 effects: Basin Research, v. 6, p. 115-130.
1387
1388 O'Reilly, C., Fallick, A.E., Jenkin, G.R.T., Feely, M., and Alderton, D.H.M., 1997a, fluid inclusion and
1389 stable isotope study of 200 Ma of fluid evolution in the Galway Granite, Connemara, Ireland:
1390 Contributions to Mineralogy and Petrology, v. 585, p. 120-142.
1391
1392 O'Reilly, C., Feely, M., Holdstock, M.P., and O'Keefe, W.G., 1997b, Fluid inclusion study of the
1393 unexposed Kentstown Granite, Co. Meath, Ireland: Transactions of the Institution of Mining and
1394 Metallurgy, v. 107, B31-37.
1395
1396 Patterson, J.M., 1970, Geology and mineralisation of the Keel area, Co. Longford, Ireland: Unpub.
1397 Ph.D. thesis, Univ. London, 274 p.
1398
1399 Peace, W.M., 1999, Carbonate-hosted Zn-Pb mineralisation within the Upper Pale Beds at Navan,
1400 Ireland: Unpub. Ph.D. thesis, Univ. Melbourne, 284 p.
1401
1402 Peace, W.M., Wallace, M.W., Holdstock, M.P., and Ashton, J.H., 2003, Ore textures within the U lens
1403 of the Navan Zn-Pb deposit, Ireland: Mineralium Deposita, v. 38, p. 568–584.
1404
1405 Philcox, M.E., 1984, Lower Carboniferous lithostratigraphy of the Irish Midlands: Dublin, Irish
1406 Association for Economic Geology, 89 p.
1407
1408 Phillips, W.E.A., and Sevastopulo, G.D., 1986, The stratigraphic and structural setting of Irish mineral
1409 deposits, in Andrew, C.J., Crowe, R.W.A., Finlay, S., Pennell, W.M., and Pyne, J., eds., Geology and
1410 genesis of mineral deposits in Ireland: Dublin, Irish Association for Economic Geology, p. 1-30.
1411

1412 Probert, K., 1983, Fluid inclusion data from carbonate hosted Irish base metal deposits [abs]: Mineral

1413 Deposits Studies Group Annual Meeting, Programme with Abstracts, University of Manchester,

1414 Manchester, UK.

1415

1416 Reed, C.P., and Wallace, M.W., 2001, Diagenetic evidence for an epigenetic origin of the Courtbrown

1417 Zn-Pb deposit, Ireland: Mineralium Deposita, v. 36, p. 428-441.

1418

1419 Rejebian, V.A., Harris, A.G., and Huebner, J.S., 1987, Conodont color and textural alteration; an index

1420 to regional metamorphism, contact metamorphism, and hydrothermal alteration: Geological Society

1421 of America Bulletin, v. 99, p. 471-479.

1422

1423 Rizzi, G., and Braithwaite, C.J.R., 1997, Sedimentary cycles and selective dolomitization in limestones

1424 hosting the giant Navan zinc-lead ore deposit, Ireland: Exploration and Mining Geology, v. 6, p. 63-77.

1425

1426 Roedder, E., 1976, Fluid inclusion evidence on the genesis of ores in sedimentary and volcanic rocks,

1427 in Wolf, K.H., ed., Handbook of Strata-bound and Stratiform Ore Deposits; I. Principles and General

1428 Studies; Vol. 2, Geochemical studies: New York, Elsevier, p. 67-110.

1429

1430 Roedder, E., 1984, Fluid Inclusions: Mineralogical Society of America, Reviews in Mineralogy, v. 12,

1431 644 p.

1432

1433 Russell, M.J., 1978, Downward-excavating hydrothermal cells and Irish type ore deposits: importance

1434 of an underlying thick Caledonian prism: Transactions of the Institution of Mining and Metallurgy, v.

1435 87, p. B168-171.

1436

1437 Russell, M.J., 1986, Extension and convection: a genetic model for the Irish Carboniferous base metal

1438 and barite deposits, in Andrew, C.J., Crowe, R.W.A., Finlay, S., Pennell, W.M. and Pyne, J., eds.,

1439 Geology and genesis of mineral deposits in Ireland: Dublin, Irish Association for Economic Geology, p.

1440 545-554.

1441

1442 Russell, M.J., Solomon, M., and Walshe, J.L., 1981, The genesis of sediment-hosted exhalative zinc +

1443 lead deposits: Mineralium Deposita, v. 16, p. 113-127.

1444

1445 Samson, I.M., 1983, Fluid inclusion and stable isotope studies of the Silvermines orebodies, Ireland,

1446 and comparisons with Scottish vein deposits: Unpub. Ph.D. thesis, Glasgow, Univ. Strathclyde, 290 p.

1447

1448 Samson, I.M. and Russell, M.J., 1983, Fluid inclusion data from Silvermines base metal – barite

1449 deposits, Ireland: Transactions of the Institution of Mining and Metallurgy, v. 92, B67-71.

1450

1451 Samson, I.M. and Russell, M.J., 1987, Genesis of the Silvermines zinc-lead-barite deposit, Ireland:

1452 Fluid inclusion and stable isotope evidence: ECONOMIC GEOLOGY, v. 82, p. 371-394.

1453

1454 Sangster, D.F., 1990, Mississippi Valley-type and SEDEX lead-zinc deposits: A comparative

1455 examination: Transactions of the Institution of Mining and Metallurgy, v. 99, p. B21-42.

1456

1457 Slowey, E.P., 1986, The zinc-lead and barite deposits at Keel, Co. Longford, in Andrew, C.J., Crowe,

1458 R.W.A., Finlay, S., Pennell, W.M., and Pyne, J., eds., 1986, Geology and Genesis of Mineral Deposits in

1459 Ireland: Dublin, Irish Association for Economic Geology, p. 319-330.

1460

1461 Slowey, E.P., Hitzman, M.W., Beaty, D.W., and Thompson, T.B., 1995, The Keel Zn-Pb and Garrycam

1462 $BaSO_4$ deposits, Co. Longford, Ireland, in Anderson, I.K., Ashton, J.H., Earls, G., Hitzman, M.W., and

1463 Tear, S., eds., Irish Carbonate-hosted Zn-Pb Deposits, Guidebook Series, v. 21: Society of Economic

1464 Geologists, p. 227-241.

1465

1466 Stanislavsky, E. and Girtzman, H., 1999, Basin-scale migration of continental-rift brines:

1467 Paleohydrologic modeling of the Dead Sea basin: Geology, v. 27, p. 791-794.

1468

1469 Stein, M., Starinsky, A., Agnon, A., Katz, A., Raab, M., Spiro, B., and Zak, I., 2000, The impact of brine-

1470 rock interaction during marine evaporite formation on the isotopic Sr record in the oceans: Evidence

1471 from Mt. Sedom, Israel: Geochimica et Cosmochimica Acta, v. 64, p. 2039-2053.

1472

1473 Stoffell, B., Wilkinson, J.J., and Jeffries, T.E., 2004, Metal transport and deposition in hydrothermal

1474 veins revealed by 213nm UV laser ablation microanalysis of single fluid inclusions: American Journal

1475 of Science, v. 304, p. 533-557.

1476

1477 Strogen, P., 1974, The sub-Palaeozoic basement in central Ireland: Nature, v. 250, p. 562-563.

1478

1479 Taylor, S., 1984, Structural and paleotopographical controls of lead-zinc mineralization in the

1480 Silvermines ore bodies, Republic of Ireland: ECONOMIC GEOLOGY, v. 79, p. 529-548.

1481

1482   Thomas, L.J., Harmon, R.S., and Oliver, G.J.H., 1985, Stable isotope composition of alteration fluids in

1483   low-grade Lower Palaeozoic rocks, English Lake District: Mineralogical Magazine, v. 49, p. 425-434.

1484

1485   Thompson, T.B., 1992, Mineralogy and fluid inclusion analyses of the Garrycam/Keel Zn-Ba-Pb-Ag

1486   system, County Longford, Ireland: Unpublished report for Chevron Oil Field Research Company, 9 p.

1487

1488   Thompson, T.B., Hitzman, M.W., and Beaty, D.W., 1992, Paragenesis and fluid inclusions of the

1489   Lisheen Zn-Pb-Ag deposit, Co. Tipperary, Ireland [abs]: Geological Society of America, Abstracts with

1490   Programs, v. 24, p. A354.

1491

1492   Trude, K.J., and Wilkinson, J.J., 2001, A mineralogical and fluid inclusion study of the Harberton

1493   Bridge Fe-Zn-Pb deposit, County Kildare, Ireland: Journal of the Geological Society, London, v. 158, p.

1494   37-46.

1495

1496   Ulrich, M.R., and Bodnar, R.J., 1988, Systematics of stretching of fluid inclusions II: Barite at 1 Atm

1497   confining pressure: Economic Geology, v. 83, p. 1037-1046.

1498

1499   Veizer, J., Ala, D., Azmy, K., Bruckschen, P., Buhl, D., Bruhn, F., Carden, G.A.F., Diener, A., Ebneth, S.,

1500   Godderis, Y., Jasper, T., Korte, C., Pawellek, F., Podlaha, O.G., and Strauss, H., 1999, $^{87}Sr/^{86}Sr$, $\delta^{13}C$ and

1501 $\delta^{18}O$ evolution of Phanerozoic seawater: Chemical Geology, v. 161, p. 59-88.

1502

1503   Von Damm, K.L., 1990, Seafloor hydrothermal activity: black smoker chemistry and chimneys: Annual

1504   Reviews, Earth and Planetary Science, v. 18, p. 173-204.

1505

1506   Walshaw, R., Menuge, J., and Tyrrell, S., 2006, Metal sources of the Navan carbonate-hosted base

1507   metal deposit, Ireland: Nd and Sr isotope evidence for deep hydrothermal convection: Mineralium

1508   Deposita, v. 41, p. 803-819.

1509

1510   Watson, J., 1978, The basement of the Caledonide orogen in Britain: Canada Geological Survey Paper

1511   78-13, p. 75-77.

1512

1513   Wilkinson, J.J., 2001, Fluid inclusions in hydrothermal ore deposits: Lithos, v. 55, p. 229-272.

1514

1515   Wilkinson, J.J., 2003, On diagenesis, dolomitisation and mineralisation in the Irish Zn-Pb orefield:

1516   Mineralium Deposita, v. 38, p. 968-983.

1517

1518 Wilkinson, J.J., and Earls, G., 2000, A high temperature hydrothermal origin for black dolomite matrix

1519 breccias in the Irish Zn-Pb orefield: Mineralogical Magazine, v. 64, p. 1077-1096.

1520

1521 Wilkinson, J.J., Boyce, A.J., Everett, C.E., and Lee, M.J., 2003, Timing and depth of mineralization in

1522 the Irish Zn-Pb orefield, in Kelly, J.G., Andrew, C.J., Ashton, J.H., Boland, M.B., Earls, G., Fusciardi, L.,

1523 and Stanley, G., eds., Europe's Major Base Metal Deposits: Dublin, Irish Association for Economic

1524 Geology, p. 483-497.

1525

1526 Wilkinson, J.J., Everett, C.E., Boyce, A.J., Gleeson, S.A., and Rye, D.M., 2005a, Intracratonic crustal

1527 seawater circulation and the genesis of sub-seafloor Zn-Pb mineralization in the Irish orefield:

1528 Geology, v. 33, p. 805-808.

1529

1530 Wilkinson, J.J., Eyre, S.L., and Boyce, A.J., 2005b, Ore-forming processes in Irish-type carbonate-

1531 hosted Zn-Pb deposits: Evidence from mineralogy, chemistry and isotopic composition of sulfides at

1532 the Lisheen Mine: ECONOMIC GEOLOGY, v. 100, p. 63-86.

1533

1534 Wilkinson J.J., Collins, S.J., and Jeffries, T., 2007, The composition of Irish-type Zn-Pb ore fluids, in

1535 Andrew, C.J. et al., eds., Digging Deeper, Proceedings of the 9th Biennial SGA Meeting: Dublin, Irish

1536 Association for Economic Geology, p. 279-282.

1537

1538 Wilkinson, J.J., Stoffell, B., Wilkinson, C.C., Jeffries, T.E., and Appold, M.S., 2009, Anomalously metal-

1539 rich fluids form hydrothermal ore deposits: Science, v. 323, p. 764-767.

1540

1541 Wright, W.R., Johnson, A.W., Shelton, K.L., Somerville, I.D., Gregg, J.M., 2000, Fluid migration and

1542 rock interactions during dolomitisation of the Dinantian Irish Midlands and Dublin Basin: Journal of

1543 Geochemical Exploration, v. 69-70, p. 159-164.

1544

1545 Yardley, B.W.D., 2005, Metal concentrations in crustal fluids and their relationship to ore formation:

1546 Economic Geology, v. 100, p. 613-632.

Table 1. Summary of microthermometric data from the Irish Orefield.

Location	Ref.	Minerals	n	Homogenization T (°C)				Salinity (wt% NaCl equivalent)				$T_m$hyd	δ^{34}S	Notes
				Mode(s)	Min	Max	Spread	Mode(s)	Min	Max	Spread			
DEPOSITS														
Abbeytown	1	sp	3	**100-110**	105	123	18	**10-11**	10	11	1.0	-		
	1	cc	18	**130-140**	88	180	92	**12-13**, 24-25	10	25	15.0	-		Post-ore calcite-py breccia: 139-174°C, 10-13 wt%
Navan	2	-	6	**180-190**	-	-	-	**24**	20	25	5.0	-		
	3	dol, sp	40	**130-140**, 160-170	90	175	85	-	-	-	-	-		Authors concluded Th values >150°C due to stretching
	4	sp	98	**100-110**, 140-150	75	176*1	101	**5-6**, 14-15, 24-25	5.4	26.2	20.8	-23.5		Primary low Th brine inclusions in late sphalerite
	4	cc, dol, ba	85	**120-130**	73	171*2	98	7-8, **20-21**	5.6	25.2	19.6	-22.9		Monophase inclusions occur
Tynagh	5	-	303	**150-160**	80	280	200	**8**, 17	5	23	18.0	-		
	6	sp	60	**230-240**	181	243	62	**12-13**	8.1	13.5	5.4	-		Secondary low Th brine inclusions common
	6	qz (o/g), ba	150	**150-160**	106	202†	96	**10-11**, 16-17, 20-21	6.4	23.2	16.8	-		Higher S modes and monophase brine inclusions in barite
Galmoy	4, 7	sp	78	**160-170**	129	179	50	11-12, **13-14**	10.8	16.6	5.8	-22.4		
	7	dol, cc	75	**180-190**	111	228	117	**13-14**	8.8*2	20.9	12.1	-		
Lisheen	8	sp	-	-	87	240	153	-	7	20	13.0	-		
	8	dol	-	-	145	260	115	**14-16**	14	16	2.0	-		
	4, 7	sp	282	**170-180**, 200-210	139*1	210*2	71	4-5, 11-12, 13-14, **17-18**	4.0	18.1	14.1	-22.6*4		Secondary low Th brine inclusions common in sphalerite
	7	cc, dol, qz	101	**150-160**, **200-210**	123	277	154	12-13, **16-17**	5.4	24.6*1	19.2	-22.7		Abundant secondary low Th brine inclusions, rare low S inclusions
Silvermines	4	sp	52	**180-190**	148	208	60	12-13, **17-18**	12.1	19.3*1	6.8	-23.1	0.0 (sp), 7.5 (sp)	
	9, 10	sp	35	**170-180**, 190-200	155	194	39	**14-15**	9.6	16.6*3	7.0	-		Inclusions with Th in 79-130 range inferred to be secondary
	11	qz, sp, ba	-	-	190	280	90	-	-	-	-	-		Only 3 data (averages?) actually presented; T range in original ref. includes S isotope geothermometry
	9, 10	qz, cb, ba	331	170-180, **190-200**	72*2	248*1	176	15-16, **18-19**	8.3*4	27.5	19.2	-		Monophase brine inclusions predominant in barite
PROSPECTS														
Tatestown	2	-	26	**180-190**	90	210	120	**10-12**	10	12	2	-		Salinity range cited by Hitzman (1995); not given by Andrew (1993)
	2	-	48	**140-150**	130	180	50	**11**, 18	-	-	-	-		
Keel	12	sp	11	**180-190**	176	185	9	**11-12**	9.2	11.7	2.5	-		
	13	sp	-	**110-120**	117	123	6	-	17	22	5.0	-	-6.5	
	4	sp	47	**120-130**	107	192	85	**14-15**, 9-10	6.0	16.5*4	10.5	-23.9		Pale to transparent sp has Th and salinity at low end of range
	14	qz	8	**180-190**	98	196	98	**5-6**	4.4	9.1	4.7	-		Quartz post-sphalerite
Keel fault, Garrycam	15	sp	25	**~130**	110	187	77	-	18.4	24.2	5.8	-		Pale to transparent sp has low Th at low end of range
	15	dol	6	**~140**	136	159	23	-	-	-	-	-		No evidence of clathrates observed
Garrycam	15	dol, ba	-	**-**	146	286	140	**~17**	-	-	-	-		No evidence of clathrates observed
Moyvoughly	2	-	229	**190-200**	120	240	120	**9**	-	-	-	-		
Harberton Bridge	16	-	-	**~100**	-	-	-	-	-	-	-	-		
Kinnitty	17	cc	29	**60-70**	48	70	22	**15-16**	9.8	20.1	10.3	-22.1, -34.7		Abundant monophase inclusions; possible two modes in hydrate melting temperature
Cooleen	18	cc	36	**50-60**	44	76	32	**20-21**	8.7	22.5	13.8	-21.3		
	19	sp	6	**170-180**	171	212	41	**14-15**	13.9	14.9	1.0	-	5.1(sp)	Reworked sp clast has low Th population of 93-123 °C
	19	dol	39	**180-190**	129	225	96	**13-14**	10.8	17.6	6.8	-	8.5(sp), 9.2(py)	
	19	cc	34	**150-160**	95	177	82	11-12, **13-14**	4.8	14.2	9.4	-		
Rathdowney prospects	7	dol	67	180-190, **210-220**, 250-260	155	267	112	11-12, **13-14**	1.4	22.4	21.0	-22.7		High Th population at Durrow (DUR1-686)
Holycross	7	sp	23	**170-180**	156	184*4	28	10-11, **16-17**	10.4	17.9	7.5	-22.7		Four inclusions with Th in range 205-244°C
Derrykearn	20	sp	-	-	185	228	43	-	13	18	5.0	-		Only ranges given
	20	dol	-	-	157	189	32	**~14**	-	-	-	-		Only ranges given
Courtbrown	21	cc	40	**170-180**	160	190*2	30	-	-	-	-	-24.0	11.0(sp)	Interpreted by authors to be "almost certainly not represenatative of mineralization temperatures"
Pallas Green	4	sp	3	**-**	141	172	31	**16-17**	13	16.1	3.1	-24.0	11.0(sp)	Drillhole sample: MN3268.9/174.1 m
	22	cc	18	**150-160**, 130-140	94	181	87	**10-12**	-	-	-	-	10.5(sp), 11.5(gn)	Drillhole samples: MN3268.4/148.7 m, MN3268.4/115.8 m, MN3268.15/155.7 m
REGIONAL CARBONATES														
Newcastle West	23	qz	-	-	160	190	30	-	-	-	-	-		
Newcastle West	23	dol	-	-	160	200	40	**~24**	-	-	-	-		
Midlands	24	dol, cc	-	**250-260**	164	271	107	**11-12**, 16-17¥	1.4	18.9	17.5	-		Fluid Type 1; not observed in supra-Waulsortian
Midlands	24	dol, cc	-	**120-130**, 140-150§	55	209	154	2-3¥, **8-9**, 9-10§	0	16.2	16.2	-		Fluid Type 2
Midlands	24	dol, cc	-	**90-100**, 140-150§	59	170*3	111	**25-26**	17.9	35.9	18.0	-		Fluid Type 3
Midlands	4	dol	46	140-150, **190-200**	135	236	101	**12-13**	9.2	14.7	5.5	-		Coarse white dolomite
Midlands	4	dol	43	180-190, **220-230**	175	257	82	**12-13**	10.5	14.2	3.7	-		White dolomite cemented breccia (white matrix breccia-type); clathrate occasionally observed
Midlands	4	dol	90	**130-140**	81	159*2	78	**30-31**#	24.1#	32.8#	8.7	-1.7		Calcic brines in replacive dolomite: drillholes 97-3459-10, 97-2091-9, 99-2512-10, 99-2512-16, 00-2512-2
Midlands	4	pink dol	49	**90-100**, 120-130	89	137*4	48	**23-25**	23.0	28.7	5.7	-17.9		Pink dolomite: drillhole samples 97-3476-01
BASEMENT														
SW Midlands area	4, 25	sp	71	150-160, **210-220**	135*3	224	89	11-12, 13-14, **16-17**	11.2*3	18.1	6.9	-23.2		Three low Th, low S inclusions in one sample (KEL-20)
SW Midlands area	4, 25	qz, cc, dol, ba	585	**170-180**	101*12	238	137	10-11, **13-14**, 17-18	8.4*4	20.6*11	12.2	-22.7		Low Th, high S primary population in one qz sample (LAT-1); correlation between Tml and Tmhyd

*?Numbers of outliers unknown (incomplete bivariate plot)

n - Number of inclusions measured for Th; in most cases the number of salinity estimates will be less

† - Th values in euhedral ore-stage quartz at Tynagh extend up to 314°C with salinities of 7.0-24.8 wt%; high Th values in barite ignored

‡ - Modes unavailable; only ranges given

¥ - From sub-Waulsortian samples

§ - From supra-Waulsortian samples

- Salinities estimated from final ice melting temperatures using metastable extension of ice liquidus; these are underestimated by <8 % relative to NaCl-CaCl$_2$ modelling.

 - not available

References: 1. Hitzman (1986); 2. Probert (1983); 3. Peace et al. (2003); 4. This study; 5. Unknown, erroneously referenced as Boast (1981) in Andrew (1993); 6. Banks and Russell (1992); 7. Eyre (1998); 8. Thompson et al. (1992); 9. Samson and Russell (1983); 10. Samson and Russell (1987); 11. Greig et al. (1971); 12. Roedder (1976); 13. Caulfield et al. (1986); 14. Collins (unpublished); 15. Thompson (1992) cited in Slowey et al. (1995); 16. Finlow-Bates, pers. comm. in Emo (1986); 17. Trude and Wilkinson (2001); 18. Strongman (unpublished); 19. Lee (2002); 20. Unknown, cited in Hitzman and Beaty (1996); 21. Reed and Wallace (2001); 22. Crowther and Wilkinson (unpublished); 23. Mulhall (2003); 24. Johnson et al. (2009); 25. Everett et al. (1999a).

Figure Captions

Fig. 1. Simplified geological map of Ireland showing localities mentioned in the text (numbered). 1. Abbeytown; 2. Tatestown; 3. Navan; 4. Keel; 5. Garrycam; 6. Moyvoughly; 7. Ballinasloe; 8. Tynagh; 9. Newcastle West; 10. Harberton Bridge; 11. Stradbally; 12. Kinnitty; 13. Derrykearn; 14. Durrow; 15. Ballyragget No. 1 borehole; 16. Rathdowney East; 17. Lisheen; 18. Galmoy; 19. Holycross; 20. Fantane; 21. Latteragh; 22. Silvermines; 23. Birdhill; 24. Ballycar; 25. Tobermalug; 26. Castlegarde; 27. Caherconlish South; 28. Srahane West; 29. Courtbrown; 30. Meelin No. 1 borehole; 31. Rocky Island. Modified after the Mineral Deposits of Ireland map (CSA Ltd and the Geological Survey of Ireland, 1994) and Everett et al. (2003).

Fig. 2. Summary of cementation and mineralization paragenesis in the Irish Midlands Basin. Modified from Wilkinson et al. (2003) and incorporating observations from Eyre (1998), Wilkinson and Earls (2000), Gregg et al. (2001), Reed and Wallace (2001), Lee and Wilkinson (2002) and Wilkinson et al. (2005b). The area filled with the breccia symbol indicates the range of paragenetic stages that are observed incorporated as clasts in synsedimentary breccias; the light grey field indicates the approximate timing of formation of undulose, subhorizontal solution seams (broadly synchronous with the onset of main hydrothermal activity); the hatched field indicates the main period of hydrothermal activity; and the dark grey field indicates the approximate timing of late, conventional stylolites (variable orientations).

Fig. 3. Plots of homogenization temperature as a function of maximum inclusion dimension for: (A) Lower Paleozoic-hosted feeder veins; (B) Regional Lower Carboniferous carbonate cements; (C) Mineral deposits. Data from Everett et al. (1999a) and Wilkinson (unpublished).

Fig. 4. Sketches of fluid inclusion assemblages from carbonate cements illustrating consistent microthermometric properties (homogenization temperatures and final ice melting temperatures), and systematic changes in relation to crystal growth zones. (A) Fine-grained replacement dolomite hosting LP_1 fluids displaying decreasing salinity and increasing T_h during growth. (B) Medium- to coarse-grained dolomite with core hosting B_3 brines and overgrowth hosting B_2 brines. Arrows indicate growth direction; dashed lines depict growth zones. Brackets indicate anomalous T_h, possibly due to leakage.

Fig. 5. Plot of Na# ($NaCl/[NaCl+CaCl_2]$) versus total salinity (wt% $NaCl+CaCl_2$ equivalent) based on ice and hydrate melting temperatures in fluid inclusions. Fields for Lower Paleozoic vein-hosted fluids (LP_1), deposit sphalerite-hosted ore fluids (LP_2) and inferred brine compositions are shown. Possible processes controlling variations in composition are indicated (see text for details). Data from one Silvermines sphalerite sample (BH K22/188') containing brine inclusions (Samson and Russell, 1987) and average data for barite and

Group 2 and 3 inclusions from Tynagh (Banks and Russell, 1992) are also shown. Comparative Southwest England brine data are from Stoffell et al. (2004) and Dead Sea brines from Klein-BenDavid et al. (2004).

Fig. 6. Halogen systematics of Irish fluids. (A) log Br versus log Cl plot; (B) Cl/Br versus Na/Br; (C) Cl/Br versus Ca/Br. Possible mixing and exchange trajectories are shown. Dashed lines in (B) represent 25 and 50% Na loss from evaporated seawater precursors. Seawater evaporation trajectory from McCaffrey et al. (1987). Compositions of modern seawater and seawater-derived brine with an evaporation ratio of 25x are shown for reference (stars).

Fig. 7. Range of major, minor and trace element compositions of LP_1 fluids (mean values from Fantane, Latteragh, Birdhill and Ballycar; Wilkinson et al., 2005a and unpublished) normalized to an evaporated seawater precursor (prior to gypsum precipitation). This illustrates the element gains/losses undergone by partially evaporated seawater during basement circulation. A range of ocean ridge vent fluid compositions are shown for comparison, normalized to a normal seawater precursor (data from TAG, MARK-1, MARK-2 and 21°N OBS; Von Damm, 1990).
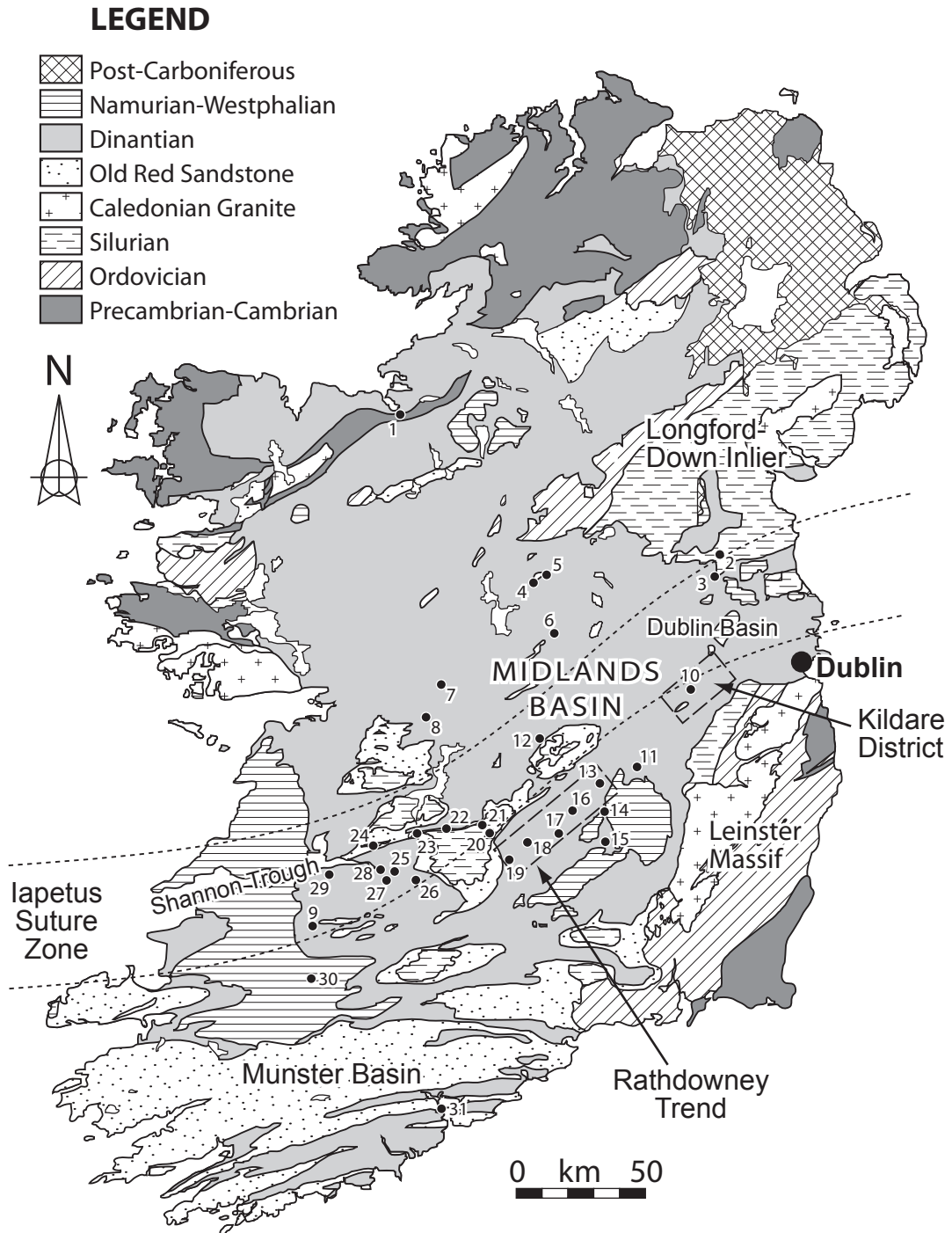
Fig. 8. Calculated $\delta^{18}O$ and measured δD compositions of water trapped in quartz-hosted fluid inclusions from Lower Paleozoic-hosted veins compared with results from Silvermines (Samson and Russell, 1987). Possible Lower Carboniferous seawater composition derived from data in Veizer et al. (1999) and assuming consistent relationship between seawater oxygen and hydrogen isotope compositions and a constant global meteoric water line. Seawater evaporation trajectory from Knauth and Beeunas (1985) and shown for both modern seawater (green) and possible Lower Carboniferous seawater (blue) starting points. Solid sausage-shaped fields indicate compositions for seawater partially evaporated to the degree inferred for the LP_1 fluids. Dashed curves illustrate modeled exchange trajectories for the extremes of the two fields, calculated at 200 and 300 °C. Range and mean Lower Paleozoic wholerock compositions from Thomas et al. (1985). Rock-fluid fractionation factors (Δ^O_{r-w} = 7.0, 3.4 at 200 and 300 °C respectively; Δ^H_{r-w} = -32.6, -33.2 at 200 and 300 °C respectively) estimated using the approach outlined in Samson and Russell (1987). Most of the LP_1 fluid compositions can be explained by small degrees of mixing between fully basement-equilibrated fluids with low δD brines, possibly produced by strong evaporation (25x evaporation ratio) of ^{18}O- and D-depleted Lower Carboniferous seawater. The higher temperature Silvermines orefluids (LP_2) do not fit the modeling implying use of inappropriate fractionation factors or, potentially, exchange with unusually low δD basement rocks.

Fig. 9. Modal homogenization temperature-salinity plot for all localities in the Irish Midlands based on the data compiled in Table 1. With a few exceptions, localities north and west of the Iapetus Suture plot in the lower left of the diagram and those from the south and east plot in the upper right suggesting a broad
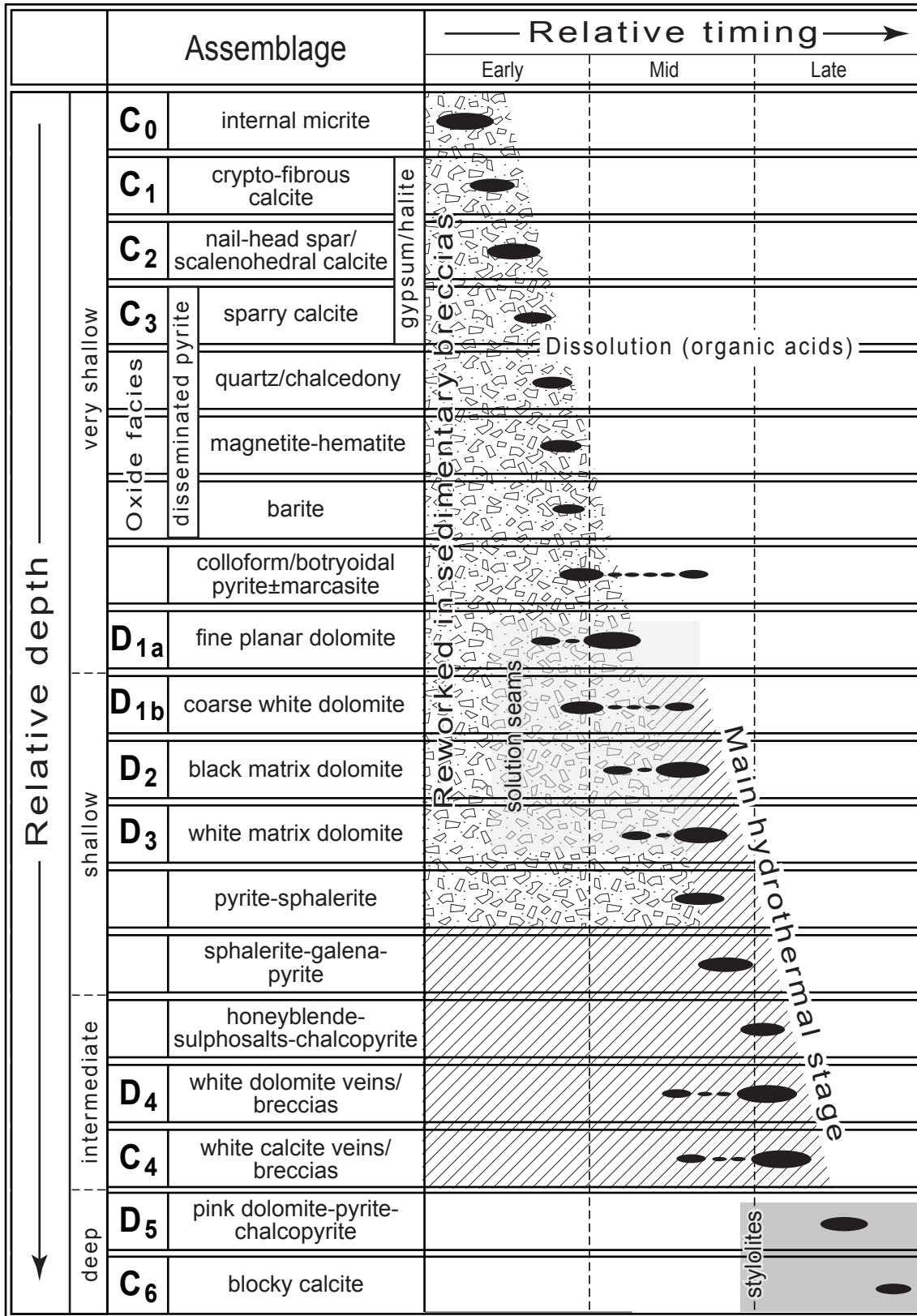
division into two main flow compartments. Exceptions are: low temperature brines at Navan that are at least partly post-ore because they occur in late stage vug-filling cements and in veins that extend far into the hanging wall stratigraphy; and high temperature, sphalerite-hosted inclusions at Tynagh (Banks and Russell, 1992).

Fig. 10. Diagrams illustrating fluid processes and controls on mineralization. A. Schematic cross-section illustrating processes responsible for generation of fluid types and chemical exchange during crustal circulation. Note approximate 2x vertical exaggeration; B. Three-dimensional cartoon representation of fault arrays, seafloor topography and mixing processes operating in the ore-forming environment. White arrows indicate possible brine migration pathways from uplifted footwall into hanging wall depressions via relay ramps; C. Representation of paleogeography in the Irish Midlands showing localization of deposits (red areas represent projection of massive sulfide lenses to the paleoseafloor) on the basinward side of fault-controlled shelves/islands where strongly evaporated bittern brines were generated.

Wilkinson_Fig. 1

LEGEND

- ⊠ Post-Carboniferous
- ☰ Namurian-Westphalian
- ▢ Dinantian
- ⋮ Old Red Sandstone
- + Caledonian Granite
- ☰ Silurian
- ⧅ Ordovician
- ▨ Precambrian-Cambrian

N

Longford-Down Inlier

Dublin Basin

● **Dublin**

MIDLANDS BASIN

Kildare District

Leinster Massif

Iapetus Suture Zone

Shannon-Trough

Munster Basin

Rathdowney Trend

0 km 50

Wilkinson_Fig. 2

	Assemblage		Relative timing →		
			Early	Mid	Late
C₀	internal micrite				
C₁	crypto-fibrous calcite				
C₂	nail-head spar/ scalenohedral calcite	gypsum/halite			
C₃	sparry calcite				
	quartz/chalcedony	disseminated pyrite — Oxide facies	Dissolution (organic acids)		
	magnetite-hematite				
	barite				
	colloform/botryoidal pyrite±marcasite				
D₁ₐ	fine planar dolomite				
D₁ᵦ	coarse white dolomite				
D₂	black matrix dolomite				
D₃	white matrix dolomite				
	pyrite-sphalerite				
	sphalerite-galena-pyrite				
	honeyblende-sulphosalts-chalcopyrite				
D₄	white dolomite veins/ breccias				
C₄	white calcite veins/ breccias				
D₅	pink dolomite-pyrite-chalcopyrite				
C₆	blocky calcite				

Relative depth ↓

very shallow / shallow / intermediate / deep

Reworked in sedimentary breccias

solution seams

Main hydrothermal stage

stylolites

Wilkinson_Fig.3

A

Decreasing salinity, increasing T_h

177
-10.7

10μm

171
-18.2

233
-6.4

186

199
-10.3

185
-7.7

183
-19.4

236
-6.4

191
-10.5

191
-8.2

191
-7.1

Sample 97-2091-5 (91.8m)
Fine-medium grained replacement dolomite. Red CL inclusion-free cores overgrown by red CL zoned, inclusion-rich bands. Late, inclusion-free, dull to non-luminescent dolomite.

B

136
-25.5

Sample 97-3459-10 (24.4m)
Dull red CL dolomite core overgrown by brighter red CL dolomite and sharp boundary with transparent dolomite that is strongly zoned in CL.

136

139

Brighter CL

127
-23.0

131
-25.2

132
-25.6

Strongly zoned
in CL with oxidized
ferroan bands

131

131

127

Dull CL

126
-31.6

124
-25.3

131
-28.2

131
-31.4

126

(152)

126
-25.3

Lower salinity, lower
Na# brine in
overgrowth

Calcic brine
in core

10μm

Wilkinson_Fig. 7

Wilkinson_Fig.9

Wilkinson_Fig.10